MITT.ÖSTERR.MINER.GES. 144 (1999)

THE DISSOLUTION BEHAVIOR OF ALBITE FELDSPAR AT ELEVATED TEMPERATURES AND PRESSURES: THE ROLE OF SURFACE CHARGE AND SPECIATION

by

Roland Hellmann

Crustal Fluids Group - Fluides et Transferts, L.G.I.T.
Université J. Fourier, CNRS, Observatoire de Grenoble, BP 53X, Grenoble Cedex 09, France
E-Mail address: Roland.Hellmann@obs.ujf-grenoble.france

Lecture to the Austrian Mineralogical Society
12th January 1998 Vienna, 13th January 1998 Graz and 14th January 1998 Salzburg

Abstract

The dissolution behavior of albite feldspar at temperatures ranging from 100–300°C and at pH ranging from 1.4 to 10.3 are presented in the form of a review of the results from HELLMANN (1994, 1995), and HELLMANN et al. (1997). The experiments were run using hydrothermal flow-through systems. The measured dissolution rates, based on Si release, represent "limiting rates" since they were measured at conditions far from albite saturation. The dissolution kinetics of albite display a strong dependence on pH, as shown by U-shaped log dissolution rate vs. pH curves at each temperature. The apparent dependence of the rates on pH increases with temperature. The measured activation energies of dissolution are higher at acid and basic pH (89 and 85 kJ mol^{-1}, respectively) than at neutral pH (69 kJ mol^{-1}). The stoichiometry of dissolution at acid pH conditions measured as a function of time shows that both Na and Al are preferentially released with respect to Si, thereby creating Na and Al leached layers. The preferential release of these elements is related to the incorporation of H into these leached layers, as shown both by solution analyses and ion beam-generated depth profiles of the near surface. Sodium and Al preferential leaching and H enrichment are processes that are pH-dependent; they decrease in magnitude with increasing pH in the acid to neutral pH region.
The dissolution behavior of albite is investigated within the context of surface complexation theory. Surface titrations of albite powders at 25°C were carried out in order to determine the surface charge as a function of pH. The H^+ and OH^- adsorption isotherms show that albite surfaces carry increasingly net positive and net negative charge at pH < 6 and pH > 10, respectively. The pH region from 6–10 corresponds to the region of minimum surface charge for albite; the exact pH of surface neutrality (pH_{ZPC}) is a function of the chemical composition of the titrating fluid as well as the specific characteristics of the albite surfaces.

The surface charge and speciation of albite surfaces as a function of pH is used to interpret the following observed dissolution behavior of albite and other feldspars: dissolution rate vs. pH, preferential leaching of Al, H penetration of leached layers, and relative dissolution rates of the plagioclase feldspars. The application of surface complexation theory with respect to the above dissolution phenomena underlines the importance of charged surface and near-surface groups, as well as the speciation of these groups.

Introduction

The evolution of the lithosphere can, in a simplified manner, be thought of in terms of positive and negative crustal processes. Positive processes can be considered to be the creation of crust at mid-ocean ridges and the formation of folded and thrusted mountain terranes and volcanic arcs at zones of plate convergence. Negative processes, on the other hand, lead to the destruction of crust. The most obvious example of this occurs in subduction zones, where cool, rigid lithospheric plates are resorbed into the asthenosphere. Perhaps less dramatic, but nonetheless also of great importance, is the breakdown of crustal rock by physical and chemical processes.

Physical processes encompass the mechanical fragmentation and the subsequent erosion and transport of crustal materials at the surface. Chemical processes generally involve the interaction of aqueous fluids with rocks, leading to their breakdown by way of the decomposition and/or transformation of their constituent minerals. Water-rock interactions span a wide variety of environments within the crust. In terms of increasing temperature and pressure conditions, water-rock interactions occur in the following generalized geological environments: chemical weathering reactions at the Earth's surface, diagenetic reactions in sedimentary basins and in subduction zones, hydrothermal reactions in the shallow crust (< 20 km), and finally, metamorphic reactions at similar or even greater depths.

The chemical reactions which define water-rock interactions have many broad implications. Perhaps most importantly, they control to a large degree the composition of natural waters, these including rivers, lakes, and oceans, as well as subsurface waters, ranging from near-surface ground waters to much deeper hydrothermal systems. At the Earth's surface, the development and evolution of soils is in large part regulated by water-rock interactions. These interactions also regulate the long-term acid-neutralizing capacity of soils and the availability of plant nutrients. With respect to the subsurface, the formation of ore and mineral deposits is in large parts controlled by the chemical nature of water-rock interactions, both in terms of dissolution and precipitation processes.

The increasingly important question of climate control and atmospheric CO_2 is also related to rock-water interactions, since the weathering of silicate rocks is now recognized as a possibly important mechanism for the removal of atmospheric CO_2, especially over multimillion-year time scales (BERNER, 1992). The following example, based on the dissolution of plagioclase feldspar and concomitant formation of kaolinite (BERNER, 1992; see original references therein), shows that increased levels of chemical weathering lead to an increased degree of CO_2 removal from the atmosphere by production of HCO_3^- ion:

$$2CO_2 + 3H_2O + CaAl_2Si_2O_8 \rightarrow Al_2Si_2O_5(OH)_4 + Ca^{2+} + 2HCO_3^- \quad (1)$$

In the realm of industrial and technical applications, water-rock interactions also play many important roles. The long-term underground burial of glass-encapsulated radwastes at acceptably low levels of risk, for example, relies on the accurate forward modeling of glass-water interactions. In addition, a comprehensive understanding of the long-term geological stability of potential underground storage sites requires extensive knowledge of the chemical and physical nature of the fluids that circulate within the host rock formations; here again, water-rock interactions play a key role. Other industrial and technical applications of rock-water interactions include such domains as petroleum extraction (oil reservoirs, oil shales, etc.), geothermal power development, in-situ mining and mine waste leaching, concrete durability, and acid rain destruction of historical monuments.

The study of water-rock interactions either in the laboratory, field, or via computer models is not a simple undertaking. Understanding the behavior of rocks in contact with an aqueous solution requires knowledge of how the individual component minerals interact. This requires the detailed study of individual mineral-water interactions in the laboratory; this is a fundamental and necessary precursor to the understanding the overall complexity of rock-water interactions.

In choosing an appropriate mineral for water-mineral investigations, the feldspar minerals are an appropriate choice due to their widespread occurrence in all types of crustal rocks (≈ 40–60 volume % in crust: ANDERSON, 1989). Albite is frequently used in experimental studies due to its pure end member composition, extensive characterization in the mineralogical literature, and ease of availability. Experiments investigating the dissolution behavior of feldspars date back to the middle of the 19th century. The first modern-day approach to feldspar dissolution studies was carried out in the 1930's (TAMM, 1930; CORRENS & VON ENGELHARDT, 1938). During the past few decades, much experimental work has been dedicated to feldspar dissolution, especially at ambient, room temperature conditions. Perhaps no other mineral has been so intensively studied with respect to mineral-water interactions. On the other hand, relatively few studies have been carried out at temperatures above 100°C (for a detailed review of the feldspar dissolution literature, see HELLMANN, 1994).

One of the main problems associated with feldspar dissolution studies at elevated temperatures is the rapid precipitation of secondary phases, thereby often making the interpretation of the experimental data problematical. On the other hand, room temperature studies have often produced kinetic data with a high degree of scatter, characterized by differences in rates of more than an order of magnitude. This is most probably attributable to the long periods of time necessary to reach steady state; few studies in the literature have convincingly reached steady-state conditions at low temperature conditions. The purpose of this article is two-fold. First, this article serves as a review of albite dissolution behavior at elevated temperatures and pressures. For the purposes of this review, data from three studies in particular are cited: HELLMANN (1994), HELLMANN (1995) and HELLMANN et al. (1997).

Where applicable, the dissolution behavior of albite in these studies is compared to those of other studies concerning both albite and other feldspars, as well. The second purpose of this article is to link various aspects of the dissolution behavior of albite to surface adsorption processes. In order to fulfill this goal, a series of surface titration experiments were carried out at 25°C using albite powders. The measured H^+ and OH^- adsorption isotherms as a function of pH allowed for the surface charge behavior of albite to be elucidated. Surface charge and speciation data as a function of pH are used to interpret many aspects of the observed dissolution behavior of albite and other feldspars.

Experimental Methods and Calculations

For the experimental results reported here, pure Amelia albite was used (composition in Table 1, HELLMANN, 1994). Samples, on the order of several mm on a side, were cleaved from a parent sample and then ultrasonically cleaned in alcohol. The surface area of the samples was 0.013 $m^2\ g^{-1}$, as based on the BET multipoint gas adsorption technique. The stock solutions used in the experiments were pH-adjusted with either HCl or KOH; no pH buffers were used. The chemistry of the output solutions was measured by standard analytical techniques using matrix-matched standards. The complete details on experimental procedures used can be found in HELLMANN, 1994, 1995.

The experiments were carried out with one pass circulating systems, either using a tubular flow system or a continuously stirred tank reactor (CSTR). Until recently, most kinetic dissolution experiments have been carried out using static autoclaves. The tubular flow system that was used was configured to resemble a CSTR (see Appendix, HELLMANN, 1994). There are several advantages to the use of CSTR vs. static reactors: (1) the rate of dissolution is a direct function of the output concentration of a given element (2) the affinity of the reaction and the pH of the solution in contact with the mineral remain constant during the steady-state operation of the reactor (3) on the other hand, the affinity of the reaction can be easily changed by varying the flow rate (4) the chemistry of the input stock solution is easily changed during an experiment. A schematic diagram of the CSTR flow system used is given in Fig. 1.

The dissolution rates were calculated according to two methods: mass loss and output concentration. The mass loss method gives an average dissolution rate over the entire duration of the experiment. The following formula is used to calculate the dissolution rate r in terms of mass loss (units of mol $m^{-2}\ s^{-1}$)

$$r = \frac{\Delta m}{(M)\,(t)\,(A)} \qquad (2)$$

where Δm is the difference in mass of the sample before and after the experiment, M is the formula weight of albite (262.219 g mol^{-1}), t is the experimental time in s, and A is the total surface area of the sample in m^2. Alternatively, the instantaneous rate r can be determined as a function of the output chemistry, based on the following formula:

$$r = \frac{(C_{out})\,(\vartheta_0)\,(10^{-6})}{(M)\,(\delta)\,(A)} \qquad (3)$$

where C_{out} is the output concentration of a given element in mg l^{-1}, ϑ_0 is the input flow rate in ml s^{-1}, M is the atomic weight of the element chosen, δ is the formula stoichiometric coefficient for the element chosen (Na, Al = 1; Si = 3 for pure albite), and A is the total surface area in m^2. Note that the stoichiometric coefficient normalizes the rate with respect to the element chosen; thus, the normalized elemental rates of dissolution represent the overall dissolution rate of albite.

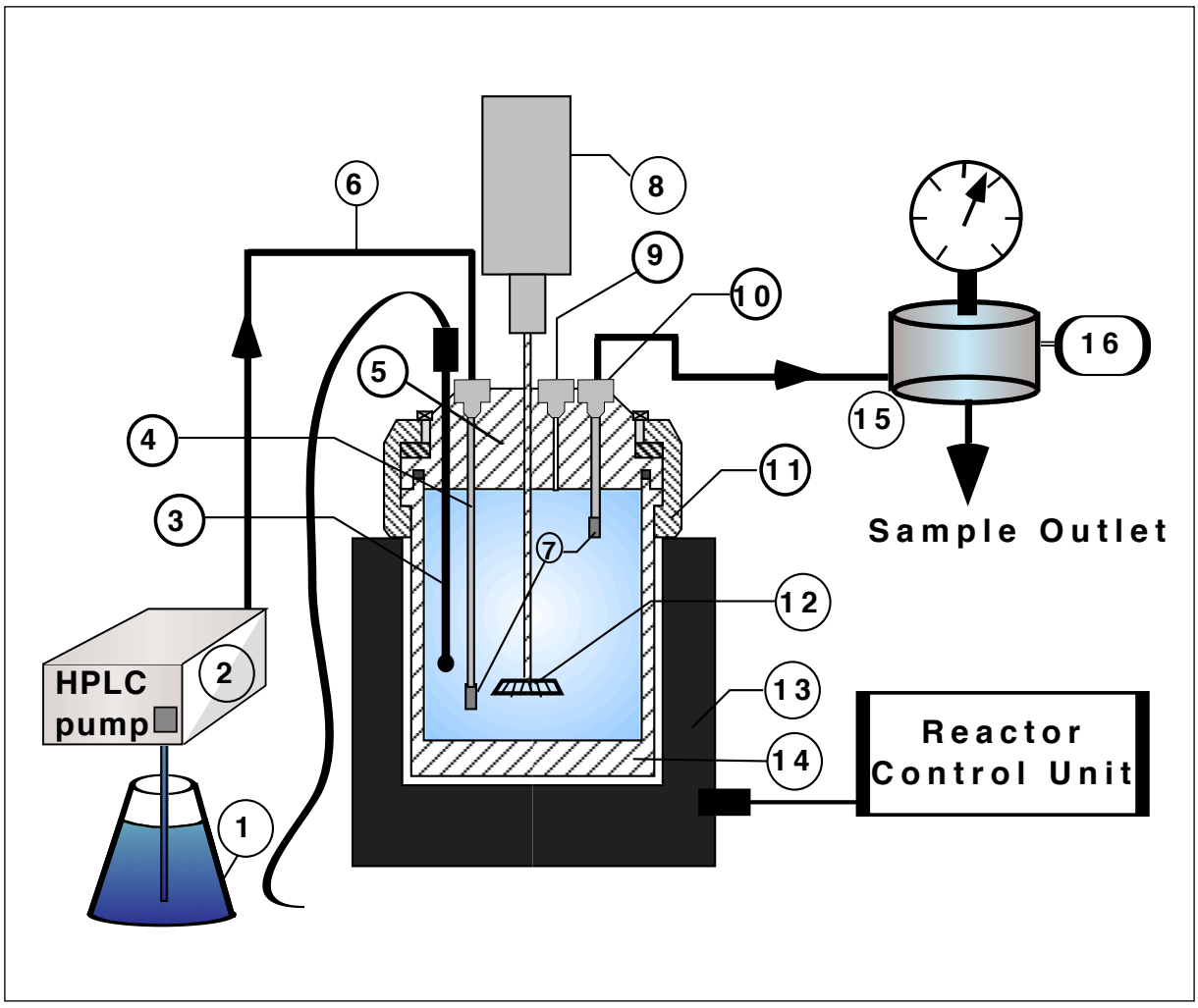

Fig. 1

Hydrothermal flow system incorporating a continuously stirred tank reactor (CSTR).
The individual components are as follows (from HELLMANN et al., 1997):
1. fluid reservoir 2. high precision HPLC pump (Knauer® series 64)
3. well for J-type thermocouple 4. inlet tubing (Ti) 5. reactor head 6. 1/8“ Ti tubing
7. 5 μm Ti filters 8. magnetic stirrer housing 9. burst disk assembly 10. Ti Swagelok® fittings
11. split ring 12. impeller 13. furnace 14. Ti autoclave, 300 ml volume (Parr® 4560 series)
15. back pressure regulator (Grove Mity Mite® S91XW) 16. high pressure gas source.

Instantaneous rates, as determined with Eqn. 3, can be representative of either non-steady-state or steady-state dissolution behavior. The initial stages of dissolution for most minerals are usually characterized by non-steady-state behavior. This type of behavior is generally transient and gives way to a steady state, where the dissolution rate remains constant over time. In addition, steady-state dissolution is often (but not always) characterized by congruent dissolution, where the relative rates of release of elements into solution reflect the stoichiometry of the elements in the solid. Thus, for albite, congruent dissolution is defined by the condition where [Na] = [Al] = 1/3[Si] in the output solution. For more details on the determination of rates, as well as steady-state vs. non-steady-state behavior, see HELLMANN (1994, 1995).

Many types of rate laws exist in the geochemical literature. A very commonly used generalized rate law, as proposed by AAGAARD & HELGESON (1982), can be written as follows:

$$r_{\text{diss}} = k_+ \Pi\ a_i^{n_{i,j}}\ f(\Delta G_{diss}) \qquad (4)$$

where r_{diss} is the overall rate of dissolution, k_+ is the forward rate constant of the dissolution reaction, a_i is the activity of the *ith* rate-determining species in the *jth* reaction, raised to some power n, and $f(\Delta G_{diss})$ is the Gibbs free energy term for the overall reaction. The Gibbs free energy term can be neglected for dissolution reactions occurring far from equilibrium (i.e. $f(\Delta G_{diss}) \approx 1$). Note that by definition ΔG_{diss} is equal and opposite to the chemical affinity of the dissolution reaction.

Results

Dissolution rates at 100, 200, and 300°C

The measured rates of steady-state dissolution at 100, 200 and 300°C, based on mass loss and Si release, are shown in Fig. 2 (data in HELLMANN, 1994). Note that the pH values shown in Fig. 2 represent the in-situ pH, as calculated by the geochemical computer code EQ3NR (WOLERY, 1983). All of the rates shown in Fig. 2 are representative of chemical affinities ranging from 64 to 238 kJ mol^{-1}. This range of chemical affinities is representative of dissolution conditions far from equilibrium, where the rate is independent of the chemical affinity. Rates that are independent from the affinity are called plateau or limiting rates (for more details concerning chemical affinities and reaction rates, as well as for a comparison with other published rates for feldspars, see HELLMANN, 1994).

There are several important points to notice with respect to the dissolution rates shown in Fig. 2. Perhaps the most important point is the strong dependence of the rates on pH at all temperatures. This U-shaped dependence of rate on pH, which is quite evident in Fig. 2, is a dissolution phenomenon that is observed for almost all minerals, and glasses, as well. There are numerous ways of expressing the dependency of dissolution rates on pH. One simple way is to divide the U-shaped dissolution rate curve, for any given temperature, into 3 separate regions corresponding to acid, neutral, and basic pH. For each respective pH region, a separate rate law for the dissolution rate r can be written as follows:

$$\text{acid pH:} \quad r = k_+ (a_{H^+})^{-n} \tag{5}$$

$$\text{neutral pH:} \quad r = k_+ (a_{H^+} + a_{OH^-})^{-n=0} = k_+ \tag{6}$$

$$\text{basic pH:} \quad r = k_+ (a_{OH^-})^{n} \tag{7}$$

where k_+ is the intrinsic forward dissolution rate constant (in theory independent of pH) and a is the activity of the given subscripted species (H^+ or OH^-) raised to an exponent n. The exponent n is a measure of the pH-dependency of the rate.

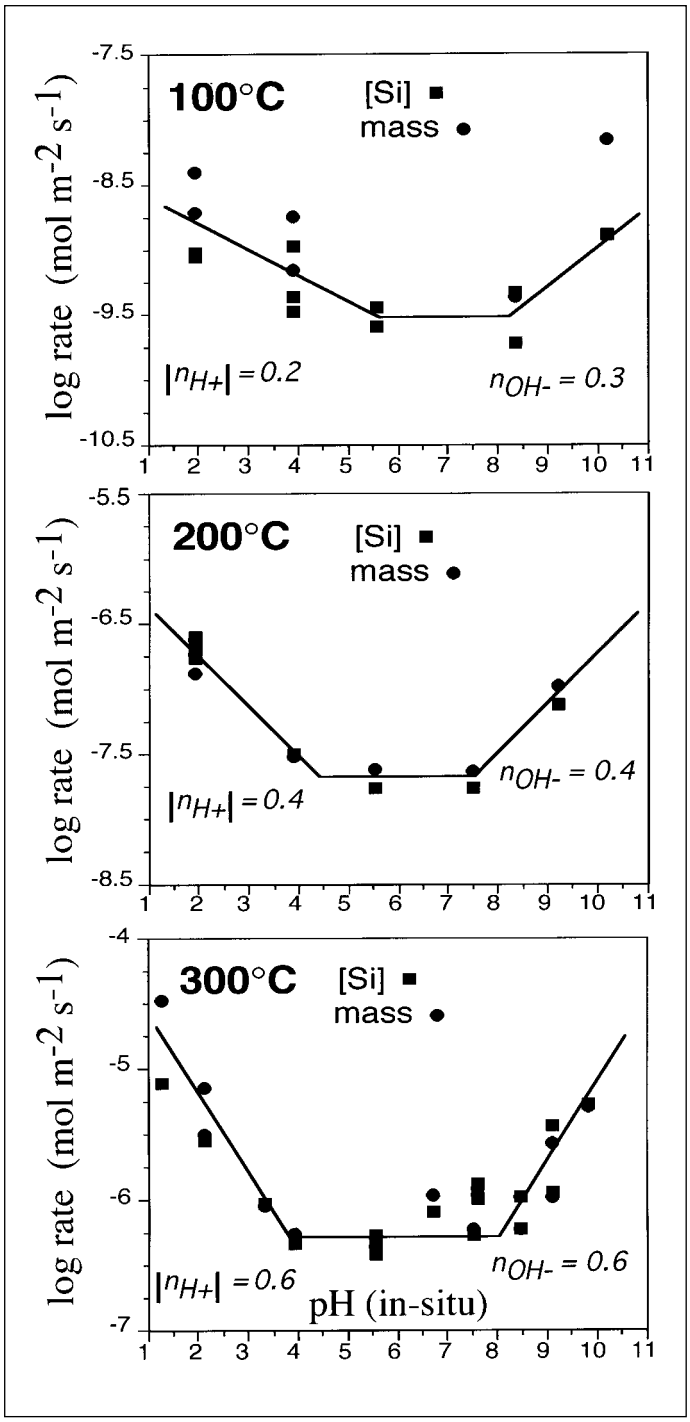

Fig. 2

Dissolution rates of albite, determined by [Si] and mass loss, as a function of the in-situ pH at 100, 200 and 300°C. The pH-dependence of the dissolution rates is described by the slope of the lines (given by $|n_{H^+}|$ and n_{OH^-}) in the acid, neutral, and basic pH regions. The apparent increase in $|n_{H^+}|$ and n_{OH^-} indicates that increasing the temperature increases the pH-dependence of the dissolution reaction at acid and basic pH conditions
(data from HELLMANN, 1994).

In Fig. 2, the rates of dissolution show no dependence on pH in the neutral and near-neutral pH range, and for this reason $n = 0$ in Eqn. 6, and as a result, the dissolution rate is equal to the rate constant k_+. On the other hand, in the acid and basic pH regions there is a linear dependence of log r with respect to pH, such that a linear regression can be used to evaluate the slope n. It is interesting to note that the absolute value of n increases with temperature (100 to 300°C), both in the acid and basic pH ranges (increasing from 0.2 to 0.6 at acid pH, increasing from 0.3 to 0.6 at basic pH – see Fig. 2; for more details, see Table 6, as well as discussion in HELLMANN, 1994).

If this increase in n is real, then this implies that the pH-dependency of the dissolution rate increases with increasing temperature. A review of aluminosilicate dissolution reactions as a function of temperature by WALTHER (1996) strongly supports this idea that the pH-dependency of dissolution rates increases with increasing temperature. The same linear regression mentioned above (i.e. log r vs. pH) can be used to calculate the values of k_+ for each pH region and each temperature. Values of k_+ are used to evaluate the temperature dependence of the overall reaction for each pH region (see Fig. 5, HELLMANN, 1994) via the classical Arrhenius relationship

$$k_+ = A \exp(-E_a / RT) \qquad (8)$$

where A is a pre-exponential factor, E_a is the activation energy, R is the universal gas constant, and T is the temperature (K). Based on Eqn. 8, the activation energies for albite dissolution are 89, 69, and 85 kJ mol^{-1} in the acid, neutral, and basic pH ranges, respectively. It is important to note that these values are more correctly called *apparent activation energies*, since they reflect the energetics associated with the entire process of dissolution (e.g. including enthalpies of H^+ and OH^- adsorption), and not just elementary bond hydrolysis reactions (for details, see CASEY & SPOSITO, 1992).

Stoichiometry of dissolution

As was mentioned earlier, the initial stages of mineral dissolution are usually characterized by non-steady-state behavior, as evidenced by dissolution rates that change rapidly as a function of time. Non-steady-state dissolution behavior is often accompanied by incongruent dissolution. Congruent and incongruent dissolution rates relate to whether or not the relative release rates of elements into solution are the same as the elemental ratios in the solid. In the case of feldspars, and citing albite in particular, the initial stages of dissolution are highly incongruent, especially at acid pH conditions. This is based on the rates of release (i.e. dissolution rates that are stoichiometrically normalized) of Na, Al, and Si measured as a function of time. An example of the transition from incongruent to congruent dissolution behavior with respect to Na and Si release rates is shown in Fig. 3; this figure also shows the concomitant transition from non-steady-state to steady-state behavior. The results that are presented below have been taken primarily from HELLMANN (1995); this study also contains a detailed review of published research concerning non-stoichiometric dissolution with respect to other feldspars. The following discussion on the stoichiometry of dissolution is limited to results in the acid and neutral pH range.

Fig. 3 shows typical dissolution behavior of albite in an acid medium. The initial dissolution rates of albite are shown, based on the normalized release rates of Na and Si. The significantly higher rate of Na vs. Si release implies that Na is stripped from the albite structure at a higher rate than Si, resulting in the formation of a near-surface structure that is depleted in Na. At acid pH conditions, Al also is released at a higher rate than Si (see Fig. 4), thereby also resulting in the creation of an Al-depleted near-surface zone. Near-surface structures that are depleted in certain elements are generally referred to in literature as altered or leached layers.

It is important to note that this type of dissolution behavior is transient for albite, since after a certain amount of time, dissolution becomes stoichiometric (i.e. congruent). In Fig. 3, congruency is evidenced by the super-position of the Na and Si release curves. In contrast, the super-position of the Na, Al, and Si curves is not achieved over the time span shown in Fig. 4, due to the lower temperature (100 vs. 200°C). It is interesting to note that while incongruent behavior is transient with albite, other feldspars, such as labradorite, apparently do not always achieve congruent dissolution behavior in laboratory studies at ambient temperatures, even over extremely long time periods (see STILLINGS & BRANTLEY, 1995).

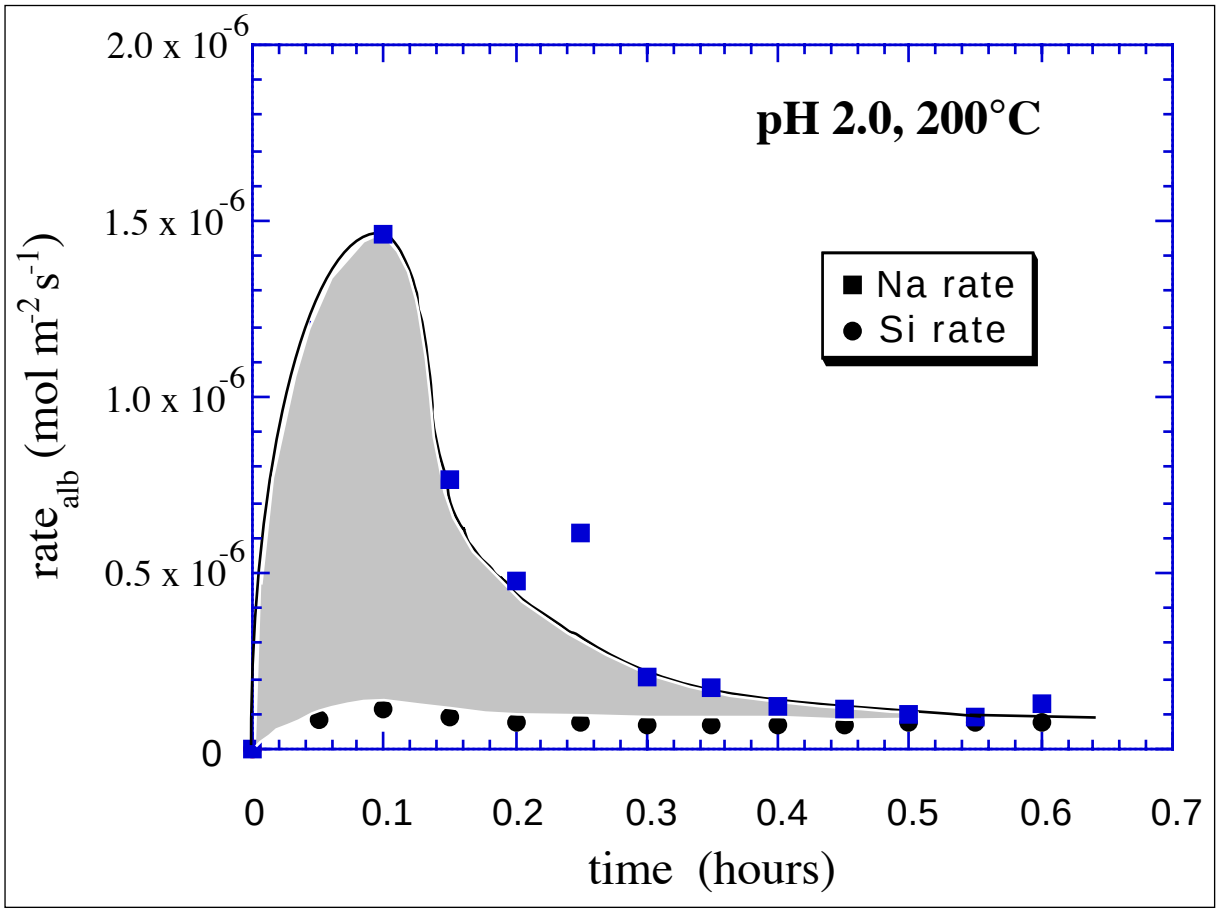

Fig. 3

The rates of Na and Si release (stoichiometrically normalized) reveal that the initial stages of dissolution are highly incongruent at acid pH conditions. The difference in the time-integrated Na vs. Si rate curves, as represented by the shaded area, indicates the formation of a Na-depleted near-surface zone. Note the attainment of steady-state, congruent dissolution after ≈ 0.6 hours (adapted from HELLMANN, 1995).

The transient nature of this non-stoichiometric dissolution is governed by two processes (see detailed explanation in HELLMANN, 1995; and original references therein): the rate of release of species from the surface (i.e. as a function of Si release, which displays conservative behavior) and the diffusion of preferentially released elements (i.e. Na and Al). When the fluxes of Na and Al diffusing from within the leached layer to the surface become equal to the surface flux of Si, the leached layers reach their steady-state thicknesses and dissolution becomes stoichiometric.

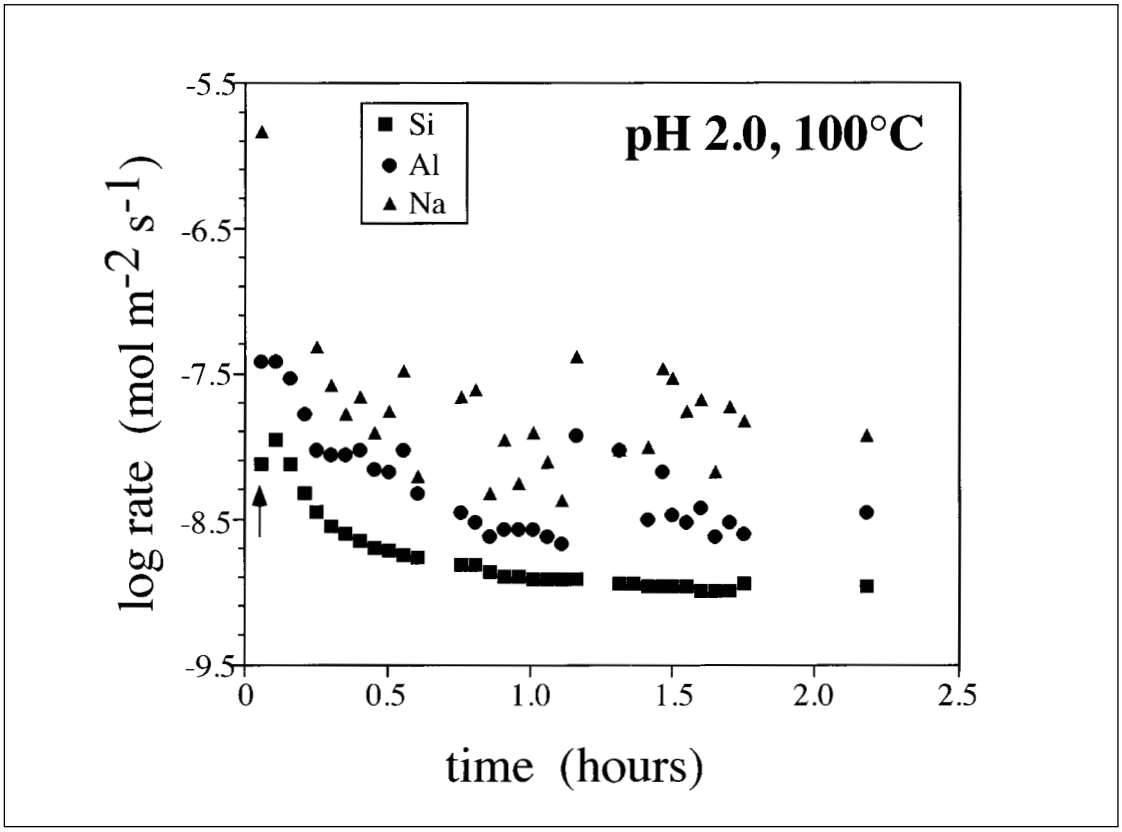

Fig. 4

Initial rates of release of Na, Al, and Si (stoichiometrically normalized) at acid pH conditions and 100°C. The higher rate of Na vs. Al release indicates that the depth of Na preferential leaching is deeper than Al preferential leaching. As in Fig. 3, depths of Na and Al preferential leaching are determined with respect to Si release rates (adapted from HELLMANN, 1995).

It is important to note that each preferentially-leached element has its own characteristic depth of depletion. For the case of albite, Na depletion depths are greater than those of Al at any given temperature and pH (see results in HELLMANN, 1995; HELLMANN et al., 1997). With respect to the feldspars and other minerals in general, the depths of elemental depletion are a function of two main variables: the mineral (structure and composition) and the fluid (composition, ionic strength, pH, temperature). Taking albite as an example, preferential leaching depths of Na and Al can range from several tens to several thousands of Å, depending on temperature, pH, and fluid composition (e.g. CHOU & WOLLAST, 1984; HELLMANN, 1995; HELLMANN et al., 1997; and references therein).

Fig. 5a shows the uptake of protons, as measured by the difference in the pH of the initial solution and the solution at the outlet of the reactor, that occurs when albite dissolves at acid pH conditions. As was the case for Na preferential release, the non-steady-state rate of H^+ uptake is a transient phenomenon, as can be noted by the achievement of a steady-state rate of H^+ uptake after several hours in Fig 5a. Fig. 5b shows the concentration of H as a function of depth from the surface of an acid pH-reacted albite; the profile shows the pervasive penetration of H to depths of > 6000 Å (note that the analytical limits of the RNRA method were exceeded).

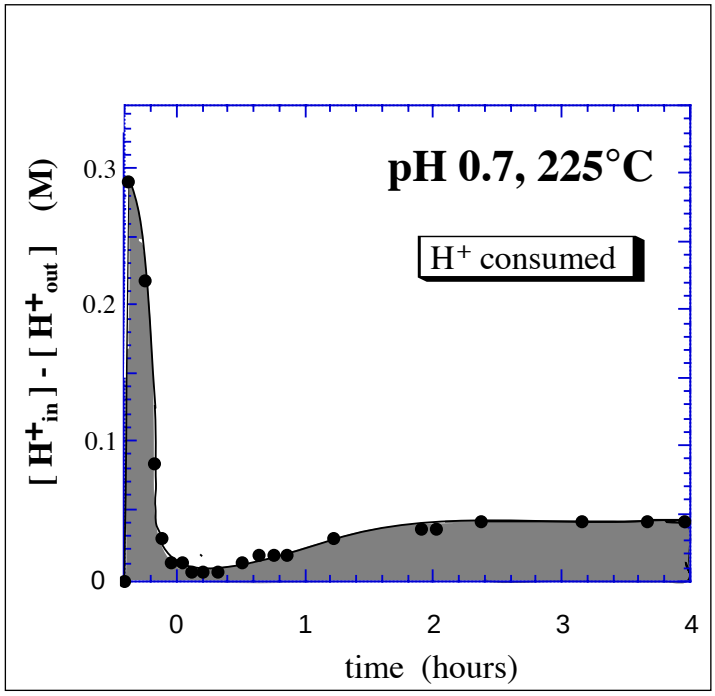

Fig. 5a

The initial stages of dissolution at acid pH conditions are also characterized by the net transfer of H^+ from the solution to the albite. This transfer of H^+ is related to the loss of Na^+ from the solid, as shown in Figs. 3 and 4, via an ion exchange process (see text for details) (adapted from HELLMANN, 1995).

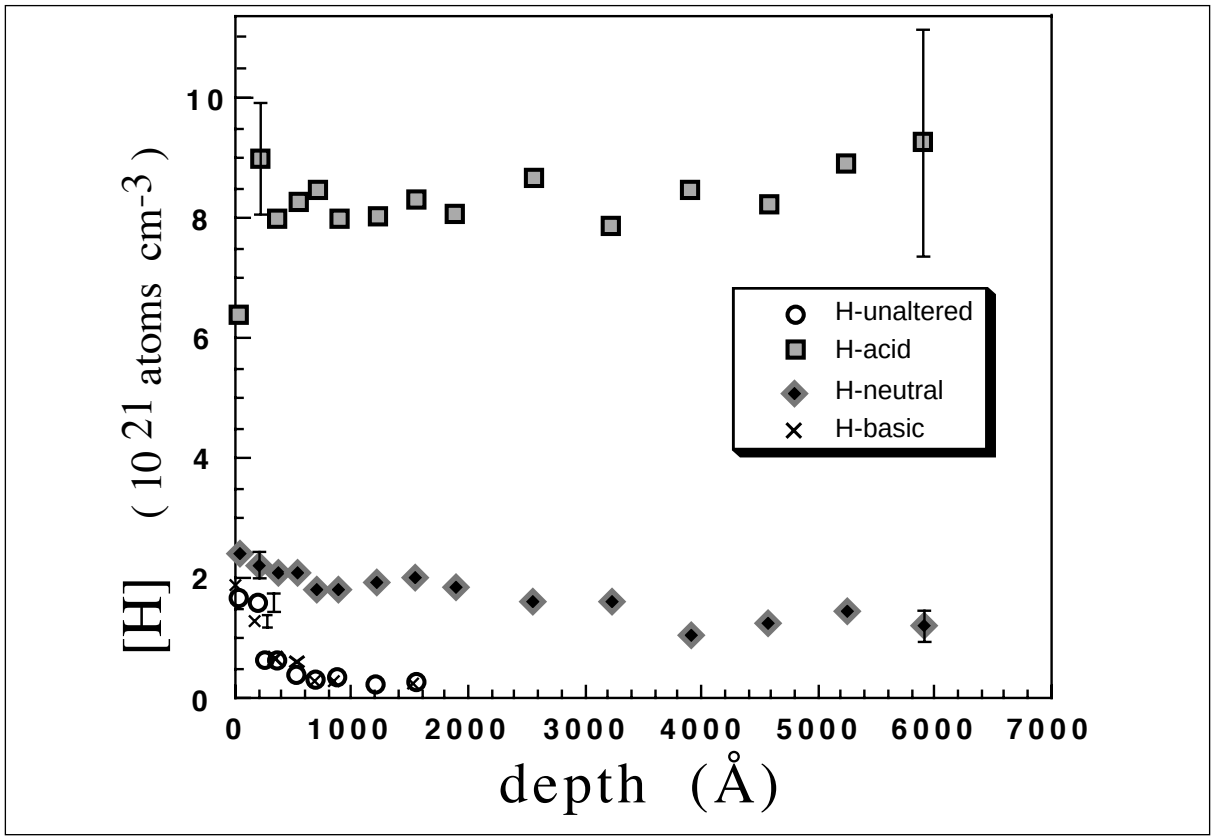

Fig. 5b

The net transfer of H^+ from the solution to the albite structure results in the incorporation of H deep into the leached layer. These depth profiles show that the penetration of H into the leached zone decreases with increasing pH. The depth profiles were measured by RNRA, an ion beam technique particularly adapted to measuring H profiles (from HELLMANN et al., 1997).

Fig. 4 and 5a,b are important in that they demonstrate that at acid pH conditions, the preferential release of Na occurs concomitantly with H uptake into the leached layer. The leaching of Na and the incorporation of H results in what is more correctly called a leached/H-enriched layer.
The concomitant leaching of Na and incorporation of H into the solid is due to a coupled ion exchange process at the surface and near surface, given by $NaAlSi_3O_8 + H^+_{aq} \leftrightarrow Na^+_{aq} + HAlSi_3O_8$. This ion exchange occurs very rapidly since Na is easily removed from the interstitial crystallographic sites where it is bound as a charge-balancing cation. It is not known, however, whether the inward diffusing species (i.e. from the solution/solid interface towards the bulk structure) is H^+ or H_3O^+, or even a combination of H^+ and H_2O (see discussion of this in HELLMANN et al., 1997). Feldspars containing other charge-balancing ions, such as Ca-rich plagioclases, undergo a similar ion exchange reaction that can be represented by: $CaAlSi_2O_8 + 2H^+_{aq} \leftrightarrow Ca^{++}_{aq} + H_2AlSi_2O_8$ (for results concerning preferential leaching and plagioclase dissolution at ambient temperatures, see for example: CASEY et al., 1988; MUIR et al., 1990; SCHWEDA et al., 1997; and references therein). Various models describing the diffusion of species within leached/H-enriched layers are treated in detail in HELLMANN (1997). It is interesting to note that there is also evidence for a limited amount of ion exchange at basic pH conditions, between surface and near-surface Na^+ (for the case of albite) and cations in solution (see evidence in HELLMANN et al., 1990, 1997).

In addition to the loss of Na due to the $Na^+ \leftrightarrow H^+$ ion exchange reaction, Al is also preferentially released at acid pH conditions during the dissolution of albite and other feldspars. Preferential Al loss has been directly measured both in terms of the stoichiometry of dissolution and by ion beam techniques for albite (CHOU & WOLLAST, 1985; HELLMANN, 1995; HELLMANN et al., 1990, 1997; and references therein), as well as for Ca-rich plagioclases (e.g. MUIR et al., 1990; SCHWEDA et al., 1997 and references therein). Fig. 4 shows an example of both Na and Al preferential release during the dissolution of albite at acid pH conditions and at elevated temperatures.
Based on elemental depth profiles generated by various ion beam techniques, the concentrations of H, Na, Ca, and Al have been measured in albite and other plagioclases after dissolution. As an example, measured H and Na profiles in albite after reaction at acid pH at 300°C show that H/Na is ≈ 2 over a depth of at least 2000 Å (see Fig. 10, HELLMANN et al., 1997). If it is assumed that H^+, and not H_3O^+, is the species that participates in the exchange reaction with Na^+ (this argument is based on the size difference of H^+ vs. H_3O^+), then this "excess" H must participate in other reactions within the leached zone. One possibility is that H species also partake in framework bond hydrolysis reactions within the leached layer (see ab initio results in XIAO & LASAGA, 1994). The study by HELLMANN et al. (1997: see Eqns. 4a, b) hypothesizes that excess H is incorporated into silanol groups that are created by the preferential hydrolysis of tetrahedrally-coordinated Al within the leached zone. This process is illustrated by the following equation (note that $Na^+ \leftrightarrow H^+$ ion exchange has already been considered in the equations below):

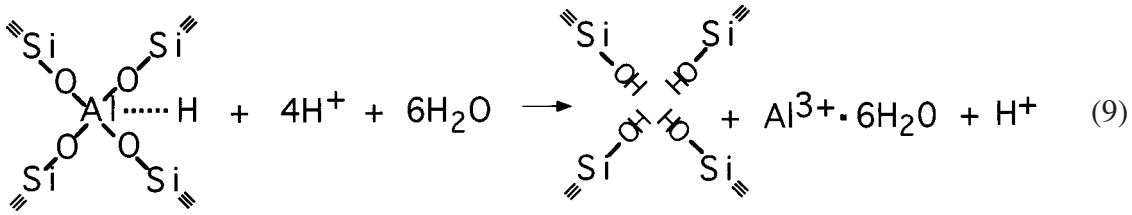

(9)

In addition to processes that serve to increase H levels in leached layers (e.g. $Na^+ \leftrightarrow H^+$ and Eqn. 9 above), others serve to decrease H levels. The process of recondensation of adjacent silanol groups (see silanol groups on right-hand side of Eqn. 9) results in the loss of H; it can be represented as follows:

$$\equiv Si\text{-}OH + HO\text{-}Si\equiv \rightarrow \equiv Si\text{-}O\text{-}Si\equiv + H_2O \qquad (10)$$

Recondensation not only results in the loss of H by the production of free water, it also serves to restructure and stabilize the leached layer by adding cross links to existing Si groups. Recondensation reactions, such as shown above, have been documented in glass dissolution studies (PEDERSON et al., 1986; BUNKER et al., 1988) and have been inferred to occur in a similar manner in leached layers formed during the dissolution of various silicate minerals (CASEY et al., 1988; PETIT et al., 1990; HELLMANN et al., 1997; SCHWEDA et al., 1997).

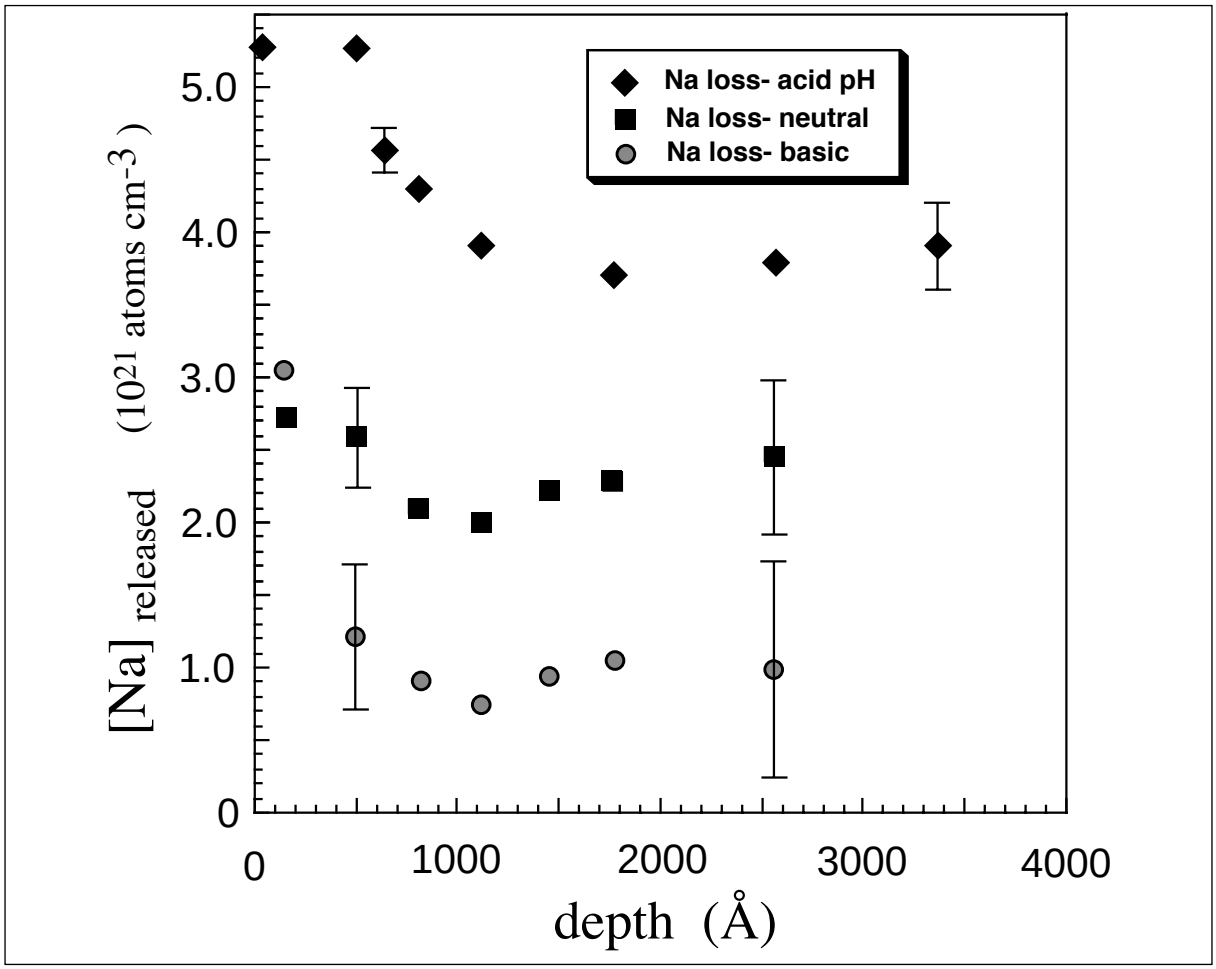

Fig. 6

Sodium loss in albite, defined as $[Na]_{bulk}$ - $[Na]_{meas.}$ as a function of pH. Note that Na loss decreases with increasing pH. The rough correlation between H incorporation and Na loss is evidence for the ion exchange relation between H^+ and Na^+ that leads to the formation of Na-depleted and H-enriched near-surface zones during dissolution at acid to neutral pH conditions. Sodium profiles were also measured by RNRA (from HELLMANN et al., 1997).

Fig. 5b shows profiles of H in albite feldspars that have been reacted at acid, neutral and basic pH conditions. This figure shows that the concentrations and depths of H penetration significantly decrease with increasing pH of the solution. The concentrations and depths of Na released (calculated on the basis of $[Na]_{bulk}$ - $[Na]_{meas.}$) after dissolution are shown in Fig. 6. Comparison with Fig. 5b shows that the pH-dependence of Na preferential release is closely related to the pH-dependence of H penetration. The preferential release of Al also decreases as a function of increasing pH from acid to neutral conditions. Nonetheless, as shown in HELLMANN (1995), the preferential leaching of Al at elevated temperatures is difficult to measure due to the rapid precipitation of Al oxy-hydroxides. Feldspar dissolution studies carried out at ambient temperatures clearly show the preferential leaching of Al vs. Si as a function of pH (e.g. CHOU & WOLLAST, 1984, 1985). The behavior of Ca and Al preferential leaching and H penetration in calcium-rich plagioclase feldspars has also been well documented via elemental depth profiles of the near surface (e.g. CASEY et al., 1988, 1989; MUIR et al., 1990; SCHWEDA et al., 1997 and references therein).

Surface Complexation Theory: a brief review

Over the past ten to twenty years, surface complexation theory has been very successfully applied to the adsorption behavior of aqueous species at the fluid/solid interface of minerals. In particular, this theory describes in mathematical terms the equilibrium adsorption of aqueous species on surfaces. Since it is generally accepted that mineral-water interactions are in large part controlled by physical and chemical processes occurring at the fluid/solid interface, this theory has received wide-spread attentionin in the past few years. As will be discussed further on, the adsorption of aqueous species, especially H^+ and OH^- on surfaces can shed important information on many of the observed characteristics of mineral-water interactions. With respect to minerals and glasses, one of the main applications of surface complexation theory is the pH-dependence of the kinetics of dissolution. With respect to albite, the feldspars, and many other aluminosilicate minerals, this theory can also be used to examine the preferential leaching of Al vs. Si at acid to neutral pH conditions, the pH-dependency of H penetration/retention in leached layers, and the relative kinetics of dissolution as applied to the plagioclase series.

The theory of surface complexation comprises not just a single theory, but rather a great number of models that describe the equilibrium thermodynamics of the adsorption of aqueous species at fluid-solid interfaces. A detailed description or review of these models is much beyond the scope of this paper (e.g. the interested reader can refer to articles in ANDERSON & RUBIN (1981), and references therein). Nonetheless, in simplified terms, most of the models differ from each other with respect to the following criteria: the types of surface species and surface reactions, the mathematical treatment of surface concentrations and mass laws, and the expression for the Coulombic term (MOREL et al., 1981).

In the current literature, three surface models standout in terms of their frequency of application (their brief descriptions below follow MOREL et al., 1981). The simplest model is called the single layer or constant capacitance model. It is based on the premise that all ions adsorb at one surface plane, all ions have the same potential, and no surface coordination of major electrolytes occurs.

The second model, also referred to as the double layer or diffuse layer model, still uses a single adsorption plane, but includes the effects of surface coordination of electrolytes within the compact layer. In addition, this model includes the effects of the ionic strength of the background electrolyte, which in turn influences the thickness of the diffuse layer that is situated between the compact layer and the bulk solution. The third model, called the triple layer model, is based on the specific adsorption of protons and hydroxide ions in an inner layer adjacent to the fluid/solid interface, while electrolytes and ligands are adsorbed in an outer layer. Both the inner and the outer layers constitute the compact layer; extending from the compact layer to the bulk solution is the diffuse layer (for a detailed analysis of these models, as well as original references, see MOREL et al., 1981). Surface complexation reactions depend on reactions between specific surface sites and aqueous species. Metal ions at the surface of a metal oxide are unstable since they are coordinatively unsaturated. Adsorption of water molecules, followed by dissociated chemisorption, results in the presence of metal-hydroxyl groups at the surface (SCHINDLER, 1981). These surface groups can be represented by >S–OH, where the ">" indicates bonding of the central metal ion *S* via bridging oxygens to the bulk structure. The simplest set of reactions are related to acid-base reactions at the surface. Surface hydroxyl groups can behave in the following manner (PARKS, 1965; SCHINDLER & STUMM, 1987):

$$>SOH + H^+_{aq} \leftrightarrow >SOH^+_2 \tag{11}$$

$$>SO^- + H^+_{aq} \leftrightarrow >SOH \tag{12}$$

Equations 11 and 12 therefore represent the protonation of a neutral and negative surface hydroxyl group, respectively. In addition to these simple acid-base reactions, surface hydroxyl groups can react with electrolytes and ligands.
The following two equations show their interaction with a negatively charged ligand L^- and a positively-charged metal ion M^+, respectively (SCHINDLER & STUMM, 1987):

$$>SOH^+_2 + L^-_{aq} \leftrightarrow >SOH_2L^0 \tag{13}$$

$$>SO^- + M^+_{aq} \leftrightarrow >SOM^0 \tag{14}$$

Similar expressions can be written that express more complex reactions involving, for example, bi-dendate ligands, etc. For each of the reactions above (Eqns. 11–14), equilibrium thermodynamic relations expressing the interaction between aqueous species and the surface can be written in terms of mass law expressions. Thus, the mass law expressions for the acid-base reactions given by Eqns. 11 and 12, respectively, can be written as:

$$K_{s,1} = \frac{a_{>SOH^+_2}}{a_{>SOH}\, a_{H^+_{aq}}}\, 10^{F\psi_0/2.303RT} \tag{15}$$

$$K_{s,2} = \frac{a_{>SOH}}{a_{>SO^-}\, a_{H^+_{aq}}}\, 10^{F\psi_0/2.303RT} \tag{16}$$

In the above two expressions, K_S represent the equilibrium constants, the *a* terms represent the activity of each subscripted species (i.e. either a surface species or an aqueous species), *F* equals the Faraday constant, *R* is the universal gas constant, and *T* is the temperature (K). The exponential term in both of the above equations represents the Coulombic interaction term; it is simply equal to the electrostatic energy necessary to bring an ion from the bulk solution to the charged surface having a given potential ψ_0. Similar mass law expressions can be written for reactions describing electrolyte and ligand interactions with surface groups (i.e. Eqns. 13 and 14).

Another useful concept associated with surface complexation theory is the pH of pristine point of zero charge (pH_{PPZC}). For a mineral surface in contact with a solution the pH_{PPZC} is the pH where the surface carries no net surface charge (the surface charge being dependent only on the adsorption of H^+ and OH^-). The definition of the pH_{PPZC} is as follows (notation from SAHAI & SVERJENSKY, 1997: $K_{s,1}$ and $K_{s,2}$ refer to the equilibrium constants defined in Eqns. 15 and 16, respectively):

$$pH_{ZPPC} = 0.5\ (\log K_{s,1} + \log K_{s,2}) \qquad (17)$$

As pointed out by SAHAI & SVERJENSKY (1997), it is difficult to measure experimentally the "true" pH_{PPZC} of a mineral due to the specific adsorption of electrolyte ions. Nonetheless, the pH_{PPZC} is a very useful physical property since the net surface charge of a mineral will be positive at $pH < pH_{PPZC}$ and negative at $pH > pH_{PPZC}$. Another more general measure of surface neutrality is called the pH of zero point of charge (pH_{ZPC}); in this case, electrolyte adsorption is not excluded.

The acid-base behavior of complex, multi-oxide mineral surfaces can often be understood in terms of the individual pH_{PPZC} or pH_{ZPC} values of analog materials. This is based on the assumption that the overall acid-base behavior of a multi-oxide surface is a function of the individual oxide surface groups. As an example, the pH_{PPZC} and pH_{ZPC} values associated with silica and aluminum oxide or oxy-hydroxides are often used to model the acid-base characteristics of >Si–OH and >Al–OH surface groups occurring on minerals and glasses.
Typical pH_{PPZC} (or pH_{ZPC}) and log $K_{s,1}$ and $K_{s,2}$ values for amorphous silica (average values calculated from original references listed in Table 1, SAHAI & SVERJENSKY, 1997), γ-Al_2O_3 (HOHL & STUMM, 1976), δ-Al_2O_3 (KUMMERT & STUMM, 1980) and γ-$Al(OH)_3$ (PULFER et al., 1984), as determined from surface titration experiments, are shown in the table below.

	log $K_{s,1}$	log $K_{s,2}$	pH_{PPZC}
am. silica	-0.7	+7.7	+3.5
γ-Al_2O_3	+7.2	+9.5	+8.35
δ-Al_2O_3	+7.4	+10.0	+8.7
γ-$Al(OH)_3$	+5.24	+8.08	+6.66

In addition to the Al-phases shown above, boehmite, diaspore, and gibbsite are also commonly used as analog minerals to model surface >Al–OH groups. These various Al phases show a large variation in pH_{PPZC} and pH_{ZPC} values, as can be noted above (see also Table II in PARKS, 1965).

All of these Al phases contain Al in 6-fold coordination (i.e. ^{VI}Al). On the other hand, Al is tetrahedrally coordinated (^{IV}Al) in feldspars. For this reason, the exact pH_{PPZC} of surface >Al–OH groups in feldspars is difficult to estimate and depends very much on which analog Al-bearing mineral is used to estimate the pH_{PPZC}. Theoretical estimates of the pH_{PPZC} of ^{IV}Al have been attempted (see PARKS, 1967).

The use of pH_{PPZC} values of monometallic oxide and (oxy)hydroxide minerals allows one to predict with relatively good accuracy the net charges associated with surface >Si–OH and >Al–OH groups on a variety of minerals. When the afore mentioned pH_{PPZC} or pH_{ZPC} values are applied to feldspar surfaces, for example, it is possible to predict that $>Al\text{-}OH_2^+$ and >Si-OH groups predominate at acid pH conditions ($pH \leq \approx 5$), giving the surface a net positive charge. Due to the log $K_{s,1}$ value for amorphous SiO_2 (≈ -0.7), >Si–OH groups will not have a tendency to protonate at low pH. At near-neutral to neutral pH conditions, the surface should have a very low net charge, due to the predominance of neutral >Al-OH and >Si-OH groups and equivalent, but low concentrations of both $>Si\text{-}OH_2^+$ and $>Si\text{-}O^-$ groups, as well as $>Al\text{-}OH_2^+$ and $>Al\text{-}O^-$ groups.

With increasing pH from neutral to basic pH conditions, the feldspar surface starts to acquire an overall negative charge, due to the increasing predominance of both $>Si\text{-}O^-$ and $>Al\text{-}O^-$ groups. According to the log $K_{s,2}$ values listed in the table above, with a shift in pH from neutral to basic pH conditions, $>Si\text{-}O^-$ groups should, nonetheless, start to form at a lower pH than $>Al\text{-}O^-$ groups. At basic pH conditions, the identity and importance (especially with respect to the kinetics of dissolution) of the predominant negatively-charged species on albite and other aluminosilicate surfaces has been the subject of debate; according to BRADY & WALTHER (1989) and WALTHER (1996), $>Si\text{-}O^-$ groups predominate, whereas BLUM & LASAGA (1991) postulate the predominance of $>Al\text{-}O^-$ groups.

Surface Titrations of Albite

Surface titrations are a convenient method for determining surface charge and surface speciation of a solid in contact with an aqueous fluid (e.g. HUANG, 1981; FORNI, 1973; and references therein). The method is based on adding discreet amounts of either an acid or a base to an aqueous suspension of a mineral powder. The composition and the pH of the suspension are continuously measured during the addition of acid or base. The concentration of adsorbed H^+ or OH^- at a given pH is calculated by the difference between the amount of acid (H^+) or base (OH^-) added to the system and the pH that is measured.

Several surface titration studies have been carried out with respect to feldspars (BLUM & LASAGA, 1988, 1991; AMRHEIN & SUAREZ, 1988; SCHOTT, 1990; UNWIN & BARD, 1992; STILLINGS et al., 1995). With the exception of the study by UNWIN & BARD (1992) the above studies are based on surface titrations that were carried out by the continuous titration of an aqueous suspension in the manner described above.

In a study by HELLMANN (submitted) a slightly different method was used. The technique consists of taking individual aliquots (1–20 ml) of CO_2-free water (which may contain a background electrolyte), and pH adjusting each aliquot with HCl or KOH, such that the aliquots have starting pH's ranging from ≈ 1–13. The pH of each aliquot is precisely measured and then a given amount of powder is added, on the order of 0.1–0.5 g. The suspension is agitated continuously to ensure efficient mixing between the suspended powder and the solution. The concentration of H^+ or OH^- adsorbed is determined as a function of the difference between the starting and final pH (a stable pH reading was generally achieved within 5 min.). The main advantage of this method is that each titration measures H^+ or OH^- adsorption on fresh, unaltered powder (this is not the case with the continuous titration method described earlier, where the surface chemistry potentially changes during the course of the titration).

It is important to note that various experimental factors may dramatically influence the adsorption behavior of H^+ and OH^-, and other species, as well. Perhaps one of the most important factors is related to the properties and characteristics of the surface, these include grinding effects, surface rugosity (e.g. step and kink density), dislocation density, ageing (time of exposure to atmosphere), presence of surface films or adventitious elements, degree of surface crystallinity, crystallographic orientation, and surface treatments (e.g. annealing at elevated temperatures, etc.). Equally important are the properties of the solution in contact with the powder: ionic strength, presence or absence of an electrolyte, and composition of the electrolyte and titrating solution. In addition to the factors listed above, the powder surface area to fluid ratio also influences the relative position of the adsorption isotherms with respect to pH. Bearing in mind the influence of the above factors, care must be taken when comparing surface titration data.

Two series of titration experiments were carried out in this study, using both unaltered and previously hydrolyzed albite powders. Fig. 7 shows a typical set of surface adsorption data for an experiment conducted with albite powder in the presence of 10^{-2} M KNO_3. The concentrations of H^+ and OH^- adsorbed show a typical "V" shape, where the data on the left-hand side represent H^+ adsorption and the creation of net positive surface charge, whereas the right-hand side data represent OH^- adsorption and the creation of net negative surface charge. The "V" trend is indicative of the net positive surface charge increasing with decreasing pH in the neutral to acid pH range, and similarly, in the neutral to basic pH range, the surface charge becomes increasingly negative with increasing pH. In the pH 6–9 range, the concentrations of adsorbed H^+ or OH^- are extremely low, this corresponding to the pH region where the albite surface has the lowest net charge, due to the predominance of >Si–OH and >Al–OH groups, and very low concentrations of adsorbed H^+ or OH^-. The concentrations of released Na, Al and Si are also shown in Fig. 7. Sodium concentrations are approximately constant over the pH range 1–10, on the order of $\approx 10^{-6}$ mol m^{-2}. In the surface titration study of albite by BLUM & LASAGA (1991), the concentration of Na released also remained constant (pH 3–8), but the Na concentrations were markedly higher ($\approx 10^{-5}$ mol m^{-2}). As shown in Fig. 7, aluminum and silicon release show a pH dependency, with minima in the neutral pH range. With the exception of the neutral and near-neutral pH range (≈ 5–9), the concentrations of adsorbed H^+ or OH^- are significantly higher than the concentrations of Na, Al, and Si released into solution. This large difference in concentrations (more than one order of magnitude) implies that corrections to $[H^+]$ or $[OH^-]$ adsorbed due H^+-Na^+ exchange or hydrolysis reactions of Al and Si species can be neglected at pH < 4 and pH > 10.

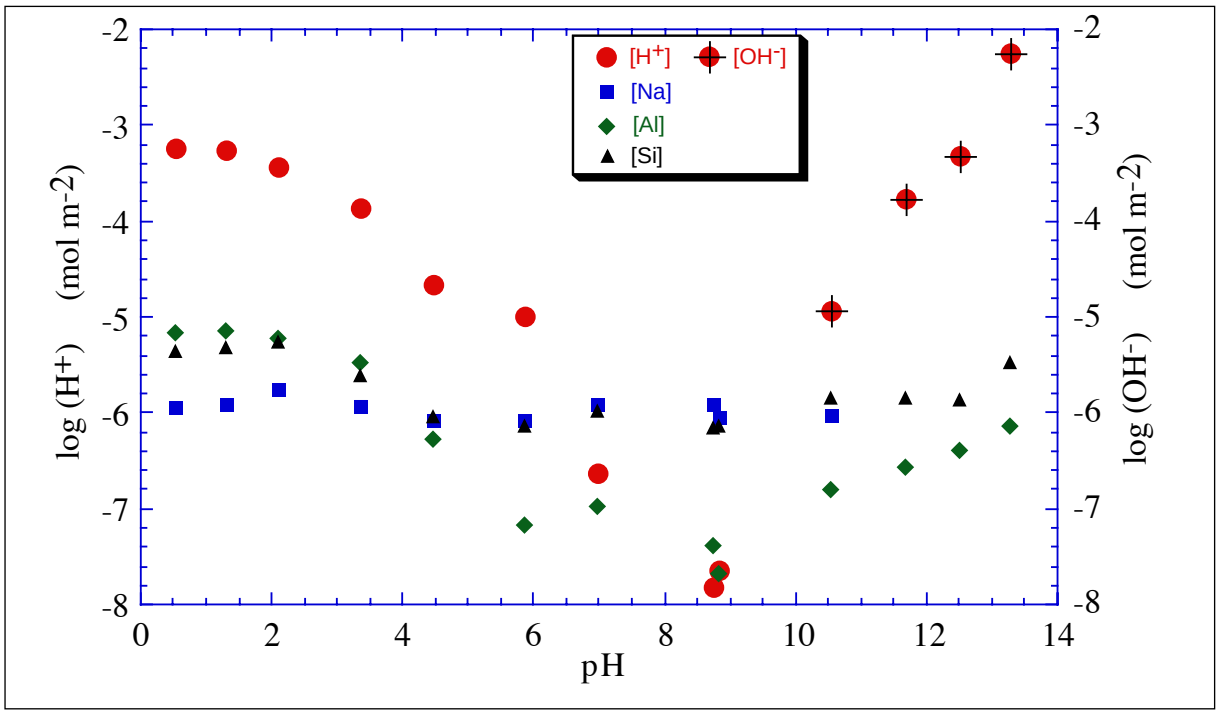

Fig. 7

A set of typical H^+ and OH^- adsorption isotherms for albite as a function of pH; also shown are [Na], [Al] and [Si] released due to dissolution. The "V" shape of the adsorption isotherms indicates increasing positive surface charge with decreasing pH (pH < 7) and increasing negative surface charge with increasing pH (pH > 10). In the pH region ≈7–9, the surface carries essentially a net neutral charge.
Note that at acid pH conditions (pH < 6), the degree of H^+ adsorption exceeds Na^+ released.
(adapted from HELLMANN, submitted)

The data from two series of surface titrations (HELLMANN, submitted) are interpreted in terms of H^+ adsorption in the acid to neutral pH range and OH^- adsorption in the basic pH range. These adsorption reactions can be examined in the context of three basic types of reactions: ion exchange, adsorption at surface >Si–OH and >Al–OH groups (see Eqns. 11, 12) and adsorption at surface bridging oxygen bonds (BLUM & LASAGA, 1991). The first type of adsorption reaction, previously discussed in detail above, is associated with the exchange reaction between H^+_{aq} and surface and near-surface Na^+ (in accordance with previous results, e.g. GARRELS & HOWARD, 1957; CHOU & WOLLAST, 1985; and references therein). This exchange reaction produces what can be termed a surface zone of hydronium feldspar (HELGESON et al., 1984). Since this reaction involves H^+_{aq} it is constrained to occur at acid to near-neutral pH conditions. It is interesting to note that in the acid to neutral pH range, there is always an excess of H adsorbed with respect to Na released (Fig. 7). This same excess of H adsorbed vs. Na released, albeit much less pronounced, has been noted in near-surface depth profiles of albite hydrothermally altered at acid pH (i.e. [H] / [Na] ≈ 2 to a depth of ≈ 3500 Å; see Fig. 10 in HELLMANN et al., 1997).

As mentioned above, adsorption of H^+ and OH^- from solution also occurs on a variety of other surface sites, namely surface >Si–OH and >Al–OH groups, as well as surface bridging oxygen sites.

The latter type of site is predicted to be very hydrophobic (ILER, 1979) and therefore is not qualitatively important (for a detailed discussion, see BLUM & LASAGA, 1991). For this reason, the following analysis of results will concentrate on the behavior of surface >Si–OH and >Al–OH sites. Correctly quantifying the adsorption behavior of these sites, however, requires knowledge of competing adsorption reactions.

As shown in Fig. 7 and based on the results from the two series of titration experiments, $[H^+]_{ads} >> [Na]$ in the pH range 1–5. Therefore, in this pH range the Na correction due to ion exchange is negligible and H^+ adsorption can be attributed to >Si–OH and >Al–OH sites (neglecting adsorption at bridging oxygen sites). On the other hand, in the neutral and near-neutral pH range (pH 5–9), the situation is much more complicated because the concentrations of adsorbed H^+ and OH^- rapidly decrease to very low levels ($< 10^{-7}$ mol m^{-2}), and in addition, their concentrations are lower than those of Na, Al, and Si (Fig. 7). In this pH region, where the surface is essentially neutrally charged, it is difficult to correct the $[H^+]$ and $[OH^-]$ adsorption data. In the basic pH region (≥ pH 9), it is not necessary to correct the OH^- adsorption data with respect to Na release, since these species do not participate in mutual ion exchange reactions. As mentioned earlier, the hydrolysis of aqueous Al species at basic pH is also of minor importance, due to the fact that $[OH^-]_{ads} >> [Al]_{aq}$.

The complete results of the two titration series are shown in Figs. 8 and 9. In both cases the data show total concentrations of H^+ and OH^- adsorbed, no corrections for Na exchange or hydrolysis reactions of aqueous species were made. The adsorption data were not combined since the first series of data was measured in solutions without a background electrolyte (Fig. 8), whereas the second series was measured in the presence of 10^{-2} M KNO_3 as a background electrolyte (Fig. 9). The samples used in both titration series came from the same parent sample, but there were, nonetheless, significant differences in sample preparation, pretreatment, and grain size. In both Figs. 8 and 9, H^+ and OH^-adsorption data on albite from BLUM & LASAGA (1991) have been included; in their study the titrations in the acid pH region were conducted in the presence of 10^{-2} M NH_4Cl.

In Fig. 8 the adsorption data corresponding to the lowest surface charge occur at pH ≈ 8–10, whereas in Fig. 9, the lowest surface charge region occurs at pH ≈ 6–8. The difference in the relative position of the low surface charge region in Fig. 8 (no electrolyte) with respect to that in Fig. 9 (10^{-2} M KNO_3) may be due to several factors, but is most probably due to the effect of the background electrolyte. It is interesting to note that in a titration study of adularia feldspar by STILLINGS et al. (1995) a series of titrations was carried out with increasing concentrations of KCl (0, 10^{-3}, 10^{-2}, 10^{-1} M KCl). Their adsorption data showed that the minimum charge region shifted from pH ≈ 9 to 7 with increasing ionic strength. As noted by STILLINGS et al. (1995), there is often confusion regarding the various definitions for the zero point of charge of mineral surfaces. For the purposes of this discussion, the general term pH_{ZPC} will be used. The pH_{ZPC} is defined to be the pH where the surface has no net charge, irrespective of the source of the charge (adsorption of H^+, OH^-, anions, cations, ligands, etc.). Thus, the data in Fig. 8 indicate a pH_{ZPC} in the pH range of ≈ 8.5–10.0. The spread in the data and pH_{ZPC} reflect several factors: titrations of albite powders having different surface characteristics and chemistries (due to pretreatments), imprecision and drift in pH measurements at low ionic strengths, and differing solid/fluid ratios.

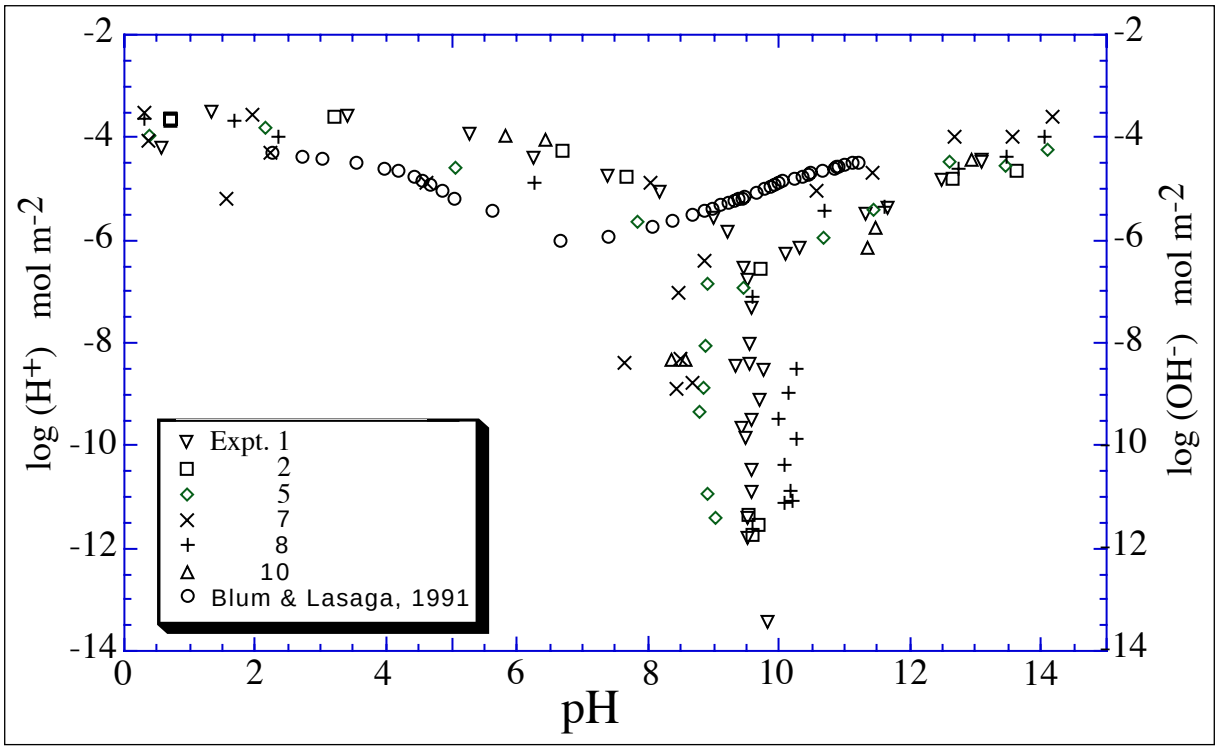

Fig. 8

H^+ and OH^- adsorption curves for albite from titration experiments carried out without a background electrolyte. The pH region where the surfaces carry a net neutral charge varies from pH ≈ 8.5–10.0. The adsorption behavior of albite from BLUM & LASAGA (1991) is shown for comparison. (adapted from HELLMANN, submitted)

The pH_{ZPC} determined from the data in Fig. 9, due to the paucity of data in the basic pH region, can effectively only be estimated from the pH where H^+ adsorption decreases sharply; this occurs at ≈ ≥ pH 6.0. As noted earlier, the adsorption isotherms in Figs. 8 and 9 were not corrected for H^+-Na^+ exchange. Correction of the H^+ isotherms for this exchange reaction results in a downward shift of the pH_{ZPC} by several pH units, to ≈ pH 5. The BLUM & LASAGA (1991) albite titration data suggest a pH_{ZPC} of ≈ 7.0 (in excess of Na^+ desorption). The values for the pH_{ZPC} (ion exchange corrected) of adularia in STILLINGS et al. (1995) vary between pH 7–9, depending on the composition and concentration of the titration medium. At any given pH, the overall concentrations of H^+ and OH^- adsorbed are often quite variable (see data in Figures 8 and 9, including those from BLUM & LASAGA, 1991), due to the reasons listed earlier. Nonetheless, several of the H^+ adsorption curves in Fig. 9 are nearly identical with the H^+ adsorption curve from BLUM & LASAGA (1991), especially at pH 4–6, where nearly all of the adsorption curves overlap. At pH < 4, the H^+ adsorption curves have a tendency to diverge from one another, this being due primarily to the adsorption curves becoming flatter with decreasing pH. Some of the adsorption curves start to flatten out at ≤ pH 4, whereas others tend to become flatter at ≤ pH 3. The flattening of the H^+ adsorption curves denotes a constancy in H^+ adsorption on the surface, perhaps due to a saturation of proton adsorption sites (BLUM & LASAGA, 1988).

It is interesting to note that this flattening out of the adsorption curves occurs in the pH range (pH 3–4) where the concentration of $>Si\text{-}OH_2^+$ groups starts to increase slowly (recalling that amorphous silica has a $pH_{PPZC} \approx 3.5$).
Nonetheless, the exact reasons for this constancy in H^+ adsorption are still not known, nor why this seems to occur over a range in pH (pH 2–4). On the other hand, the OH^- adsorption curves are relatively linear over the pH range of 10–14 (see Fig. 8; also BLUM & LASAGA, 1988).

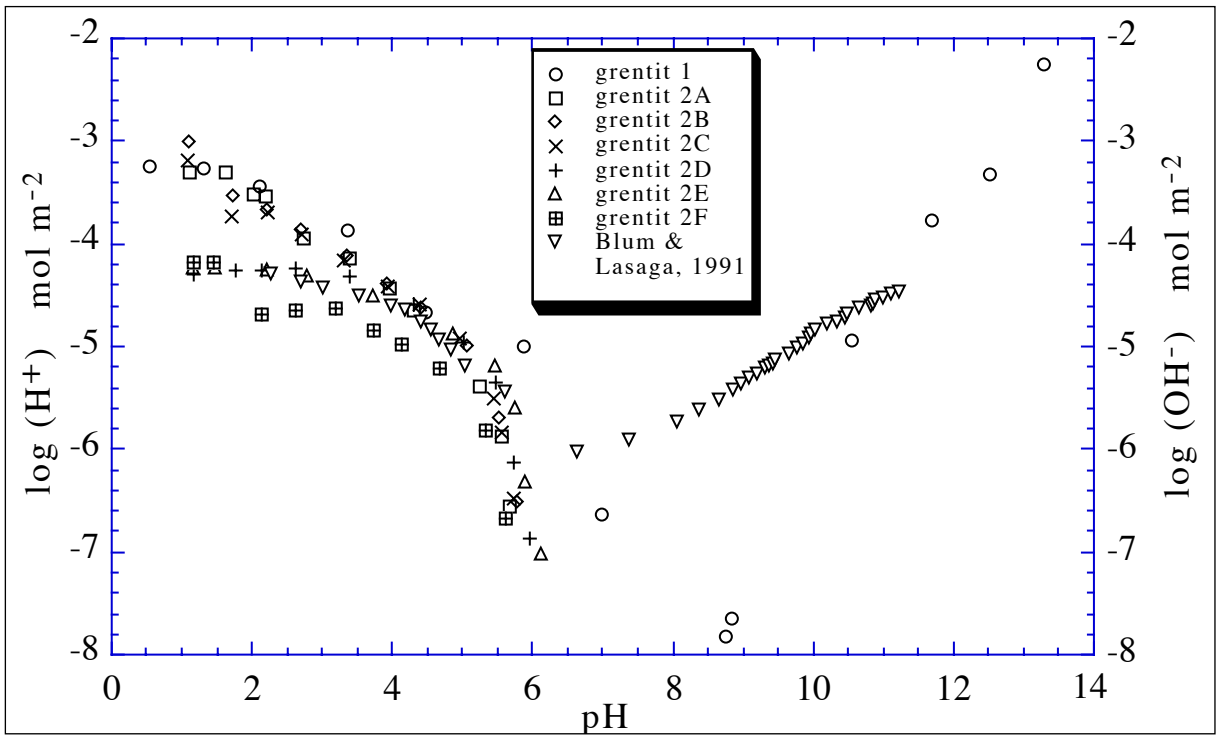

Fig. 9

H^+ and OH^- adsorption curves for albite from titration experiments carried out in the presence of 10^{-2}M KNO_3 background electrolyte. Note the pH region of net neutral charge is shifted to a lower pH (≈ 6–7) with respect to Fig. 8. The adsorption behavior of albite from BLUM & LASAGA (1991) is shown for comparison. (adapted from HELLMANN, submitted)

The dependence of H^+ and OH^- adsorption on pH is a function of the slopes determined by linear regressions of the adsorption curves shown in Figs. 8 and 9. In the acid pH range, the linear part of each H^+ adsorption curve was regressed; in general, this corresponds to the data ranging from pH ≤ 4–5 to the pH where the adsorption curve starts to flatten out. Evaluation of the pH-dependence of the H^+ adsorption data for non-altered albite (Figs. 8 and 9) yields slopes ranging from -0.18 to -0.48 (avg. -0.34); for altered albite the slopes range from -0.25 to -0.44 (avg. -0.32). In the basic pH range, the OH^- adsorption curves were regressed in the region pH ≥ 10. The pH-dependence of the OH^- adsorption data for non-altered albite (Figs. 8 and 9) yields slopes ranging from +0.60 to +0.94 (avg. +0.82); for altered albite the slopes range from +0.39 to +0.58 (avg. +0.51). In comparison, BLUM & LASAGA (1988, 1991) report pH dependencies for albite of -0.57 and -0.52 for H^+ adsorption, respectively, and +0.29 and +0.37 for OH^- adsorption, respectively. STILLINGS et al. (1995) determined a value of -0.25 for the pH-dependence of H^+ adsorption on adularia feldspar.

Discussion

The relation between surface charge and the detachment of metal atoms from surface sites is of crucial importance in understanding many aspects of mineral dissolution kinetics and behavior. In a study of the dissolution of Fe oxides, ZINDER et al. (1986) suggested a dissolution rate law where the rate is proportional to the concentration of adsorbed protons on the surface. These authors argue that proton absorption results in the polarization and weakening of the surface metal-oxygen bonds. In addition, the above study proposes that proton adsorption, coupled with electron reduction of the metal center, are the key steps in the dissolution of all oxides. Much work over the past decade has been done trying to relate surface charge and speciation to the observed kinetics of dissolution of various minerals and glasses. In the discussion below, the importance of surface charge and speciation is examined as it applies to various aspects of dissolution behavior applied to albite and other feldspars.

Dissolution rate and pH

Studies of proton adsorption on oxide surfaces (e.g. ZINDER et al., 1986; STUMM & FURRER, 1987; and references therein) have drawn attention to the influence that surface charge exercises on the rate of surface metal detachment and the overall dissolution rate. It appears that almost all mineral and glass studies in the literature show a U or V-shaped relationship between surface charge and pH (note that the exact shape of the adsorption curve is dependent on whether log surface charge or simply surface charge is plotted as a function of pH). Quite interestingly, the dissolution behavior (i.e. rate) of most minerals and glasses also displays a very similar U-shaped relationship with respect to pH. It is this qualitative resemblance in the adsorption and rate curves as a function of pH that is suggestive of a strong link between adsorption and dissolution behavior.

Taking the specific example of albite dissolution, both at elevated temperatures (see Fig. 2) and at 25°C (e.g. CHOU & WOLLAST, 1985), the rate of albite dissolution is strongly pH-dependent: it increases with decreasing pH in the acid pH region, and it increases with increasing pH in the basic pH region. The pH-dependence of this relationship is expressed in terms of the exponent n associated with the activity terms for H^+ and OH^-, respectively, in the overall rate law (see Eqns. 5, 7). Therefore, the rate r can be expressed in terms of $r \propto a_{H^+}^{-n}$ and $r \propto a_{OH^-}^{+n}$ in the acid and basic pH regions, respectively. With increasing temperature (100 - 200 - 300°C), n was found to vary from -0.2 to -0.6 in the acid pH region while in the basic pH region, n varied from 0.3–0.6 (HELLMANN, 1994). In comparison, CHOU & WOLLAST (1985) determined that $n = -0.5$ at acid pH and $n = 0.3$ at basic pH and 25°C. It is important to note that temperature may effect the value of n over a given pH range, such that a comparison of n between various temperatures is not rigorous.

Surface titration data allow for the determination of surface charge and speciation as a function of pH. Since surface titrations are not (yet) feasible at temperatures > 100°C, only data from low temperature surface titrations are currently available. Based on the titration results at 25°C in the study by HELLMANN (submitted), the average slopes of the data (from Figs. 8 and 9) representing log $[H^+]$ adsorbed vs. pH are -0.34 and -0.32 for unaltered and altered albite, respectively; the average slopes of the log $[OH^-]$ vs. pH adsorption isotherms are +0.82 and +0.51, for unaltered and altered albite, respectively.

To compare, BLUM & LASAGA (1988, 1991) report pH dependencies for albite of -0.57 and -0.52 for H^+ adsorption, respectively, and +0.29 and +0.37 for OH^- adsorption, respectively. With the exception of the log [OH^-] vs. pH dependency for unaltered albite in the study of HELLMANN (submitted), the slopes mentioned above correspond moderately well with the respective acid and basic pH slopes associated with log dissolution rate vs. pH data for albite dissolution at 25°C in the literature. As an example, the albite study of CHOU & WOLLAST (1985) reports log rate vs. pH data in the acid and basic pH regions with slopes equal to -0.49 and +0.30, respectively. In addition, these values are not too different from the slopes of the rate vs. pH data in the acid and basic pH regions at elevated temperatures in HELLMANN (1994). For the case of K-feldspars, STILLINGS et al. (1995) determined a slope equal to -0.25 for log [H^+] adsorbed as a function of pH; these authors compare this H^+ adsorption-pH dependency with data for microcline (SCHWEDA, 1990) that yields a slope of -0.5 for log rate vs. pH data in the acid pH region.

It is interesting to note, however, that the flattening of the H^+ adsorption curves at low pH (pH < 3–4) that was noted in this study (Figs. 7–9), as well as in BLUM & LASAGA (1988, 1991), is not reflected in the corresponding dissolution rate trends at these low pH. Both at 25°C (e.g. CHOU & WOLLAST, 1985) and at elevated temperatures (Fig. 2), the rates of dissolution do not flatten out with decreasing pH, even down to pH ≈ 1. Thus, this is an example where the relation between H^+ adsorption and dissolution rate is not well understood.

Based on the overall close similarity between the slopes of their H^+ and OH^- adsorption vs. pH data and the slopes of the rate vs. pH data of CHOU & WOLLAST (1985), BLUM & LASAGA (1988) concluded that there is a simple first-order dependence of the dissolution rate of albite on the surface concentrations of adsorbed H^+ and OH^-. Thus, the dissolution rate *r* in the acid and basic pH regions, respectively, can be expressed as follows (adapted from BLUM & LASAGA, 1988):

$$r \alpha c_{S\text{-}OH_2^+}^{+1.0} \text{ at pH} < 6 \qquad (18)$$

$$r \alpha c_{S\text{-}O^-}^{+1.0} \text{ at pH} > 7 \qquad (19)$$

Based on the information discussed above with respect to the acid-base behavior of surface silica and alumina groups, the identity of the metal center *S* in Eqns. 18, 19 with respect to the feldspars can be determined. At acid pH, the rate will be proportional to the concentration of surface >Al–OH_2^+ groups, whereas at mildly basic pH conditions, the rate will be dependent on the surface concentration of Al–O^- groups or Si–O^- groups (Al vs. Si is a point of conjecture – it depends on which Al phase is chosen as an analog for >Al–OH groups: refer to discussion concerning pH_{PPZC} above, as well as discussion in BLUM & LASAGA, 1991). At extremely basic pH conditions, the charge-determining surface groups should be comprised of both >Si–O^- and >Al–O^- groups. The near-neutral pH range, where the dissolution rate data are more or less pH-independent (see Fig. 2), should correspond to a minimum in the concentration of charged groups, such as >Al–OH_2^+ , >Al–O^-, >Si–OH_2^+ and >Si–O^- surface groups, and concomitantly, a maximum in the concentration of neutral >Al–OH and >Si–OH groups (see Figs. 7–9). The correspondence between surface charge, rates of dissolution, and pH, while not perfect in all aspects, seems to hold moderately well.

In a review paper concerning the dissolution behavior of a wide variety of aluminosilicate minerals, WALTHER (1996) shows many examples of the direct relation between surface charge and speciation, pH, and dissolution kinetics. According to this aforementioned study, surface complexation theory can be broadly applied to explain many aspects of the dissolution behavior of nearly all aluminosilicate minerals (and glasses, by implication), even in chemically complex solutions. Nonetheless, the general applicability of this theory has been the subject of recent debate, as discussed in WALTHER et al. (1997).

Preferential leaching

As was discussed above, the dissolution behavior of albite, and other feldspars as well, is characterized by the preferential leaching of charge-compensating interstitial cations (Na, K, Ca), as well as Al, a framework forming element (e.g. CHOU & WOLLAST, 1984, 1985; HELLMANN et al., 1990, 1995; STILLINGS & BRANTLEY, 1995; SCHWEDA et al., 1997; and references therein). The pH-dependency of these preferential leaching phenomena is complex (see HELLMANN, 1995; HELLMANN et al., 1997), especially when considering conditions ranging from very acid to very basic pH at elevated temperatures. For the purposes of the following discussion, we will restrict ourselves to pH conditions ranging from acid and neutral. As was discussed above and shown in Figs. 3, 4, and 6, the preferential leaching of Na (or K for K-feldspars and Ca for plagioclases) is very pH-dependent (for brevity, only Na preferential leaching is considered below). This is primarily a result of the fact that this type of preferential leaching is due to ion exchange of Na^+ with H^+ (or H_3O^+) in solution (see HELLMANN, 1997 with respect to Na^+-H^+ inter-diffusion models). The degree of Na loss and H penetration into the altered/leached structure depends primarily on the respective Na and H gradients between the solution and the solid. The H gradient is a function of pH; thus, acid pH conditions favor ion exchange and the replacement of Na by H (HELLMANN et al., 1997; and references therein). Similarly, decreasing the Na gradient (e.g. by adding Na to the solution), also serves to decrease the degree of ion exchange (see results in PETIT et al., 1989).

The preferential leaching of Al vs. Si at acid to neutral pH conditions, on the other hand, is a phenomenon due to Al detachment being kinetically more favorable than Si detachment (for albite: see Fig. 4 above, HELLMANN et al., 1990, HELLMANN et al., 1997; for plagioclase: see results in SCHWEDA et al., 1997; and references therein). The primary reason for this is related to the charge associated with surface Al and Si groups. As mentioned earlier, at acid pH conditions, surface Al groups primarily occur as $>Al\text{-}OH_2^+$, whereas surface Si groups occur predominantly as neutral >Si–OH. Since the Al surface groups carry a positive charge, they are inherently more reactive and are more easily hydrolyzed. The underlying principle of Al preferential leaching is the same as was discussed for the overall rate of dissolution: the dissolution rate is proportional to the concentration of charged surface groups (i.e. $r \alpha c_{S\text{-}OH_2^+}$ at acid pH conditions).

Recalling that Al preferential leaching decreases with increasing pH (see discussion above), this pH-dependency can be explained by the decreasing concentration of positively-charged $>Al\text{-}OH_2^+$ groups as the pH approaches neutrality. Thus, at neutral or near-neutral pH conditions, >Al–OH and >Si–OH groups predominate, and hence Al detachment rates should become roughly equal to those of Si.

In reality, the degree of Al preferential leaching does not completely vanish, this being due to the fact that >Al–O_{br} bonds are slightly longer (and therefore weaker) than >Si–O_{br} bonds (GEISINGER et al., 1985), where O_{br} denotes a bridging O bond between two metal atoms. Nonetheless, as shown by the results in HELLMANN (1995) and HELLMANN et al. (1997), Al and Si detachment rates in albite at neutral pH and elevated temperatures can, within the error of analysis, be considered to be roughly equal, with no appreciable Al leached layers forming. A very similar result is shown at 25°C in the albite dissolution study of CHOU & WOLLAST, 1994, 1995.

H penetration of leached layers

In the neutral to acid pH range, H penetration into the leached/altered zone of albite increases with decreasing pH (see Fig. 5b). This trend has also been found in other feldspars, such as the plagioclases (CASEY et al., 1988, 1989; SCHWEDA et al., 1997; and references therein). As discussed above, this can be attributed to the ion exchange reaction between Na^+ (Na^+ and/or Ca^{2+} for the plagioclases) in the near-surface structure and H^+ (or H_3O^+) in solution. Even though this process can be thought of as being predominantly responsible for the incorporation of H into the leached/altered zone, the preferential leaching of Al may also play a role (see details in HELLMANN et al., 1997).

The preferential release of Al from the near surface is responsible for the creation of Al depleted layers, as discussed above and shown schematically in Eqn. 9. According to the formulation in Eqn. 9, the preferential hydrolysis of tetrahedrally coordinated Al atoms results in the creation silanol groups; more precisely, the hydrolysis and removal of one tetrahedrally-coordinated Al leaves behind 4 silanol groups (i.e. $\equiv$Si-OH), resulting in a net gain of 3 H within the leached layer. Thus, the preferential loss of Al to significant depths should result in the incorporation of significant amounts of H into the leached structure. Counterbalancing this incorporation of H into the leached structure is the process of recondensation of silanol groups, as shown in Eqn. 10.

The same arguments that apply to the preferential removal of surface Al-OH_2^+ groups at acid pH conditions are postulated to hold true for the behavior of Al–OH groups created by hydrolysis reactions within the leached layer. According to the ab initio results of XIAO & LASAGA (1994), >Al–O_{br}–Si< bonds are intrinsically more reactive than >Si–O_{br}–Si< bonds (O_{br} denotes a bridging oxygen). This translates to the hydrolysis of tetrahedrally-coordinated Al being kinetically favored with respect to the hydrolysis of tetrahedrally-coordinated Si. Hydrolysis of >Al–O_{br}–Si< bonds results in the formation of >Al–OH groups. The penetration of H^+ (or H_3O^+) into the leached layer is then postulated to result in the protonation of these >Al–OH groups, resulting in the formation of >Al–OH_2^+ groups within the leached layer. Just as is the case with respect to surface >Al–OH_2^+ groups, the positive charge on >Al–OH_2^+ groups can be envisioned to catalyze hydrolysis reactions of the remaining bonds that serve to bind >Al–OH_2^+ groups within the leached layer (i.e. the remaining bonds are denoted by the ”>” symbol). Complete hydrolysis of >Al–OH_2^+ groups within the leached layer results in the detachment and removal of Al from the leached layer.

The above scenario, while not experimentally verified, is nonetheless, a plausible explanation for the interrelationship between charge, speciation, and preferential release kinetics of Al within leached layers. The main difference between this and the preceding arguments is that these reactions occur within the near surface, leached layer zone and not directly on the surface. It is also interesting to note that the pH-dependence of Al removal (i.e. less Al is preferentially removed as pH increases) may also be related to the pH-dependence of Na removal via the ion exchange, Na^+-H^+ interdiffusion mechanism. Thus, as pH increases from acid to neutral pH conditions, less H^+ is exchanged with Na^+, thereby making less H^+ available for the preferential hydrolysis of >Al–O_{br}–Si< bonds within the leached layer.

Dissolution rates of plagioclases

Various studies have found that plagioclase composition, which varies from the albite end-member ($NaAlSi_3O_8$) to the anorthite end-member ($CaAl_2Si_2O_8$), is itself a factor in the rate of dissolution, all other experimental parameters being equal. In a study of the dissolution rates of plagioclase at pH 2 and 3, Casey and co-workers found that the rates of dissolution increased in a non-linear fashion as a function of Ca (i.e. anorthite) content (CASEY et al., 1991). Their results show that as the anorthite mole percent of the plagioclase increases from 0 to almost 100 %, the rates of dissolution increase by several orders of magnitude. Results similar to these were determined in a study of plagioclases by OXBURGH et al. (1994) and STILLINGS & BRANTLEY (1995).

The three aforementioned studies were carried out under acid to near-neutral pH conditions. Based on arguments pertaining to surface charge and speciation presented earlier, these pH conditions require that >Al–OH_2^+ and >SiOH are the predominant surface groups with respect to the entire plagioclase series. As expected for these pH conditions, preferential removal of surface >Al–OH_2^+ groups occurs in the acid pH range, due to their positive charge. As was also discussed immediately above, it is plausible that >Al–OH_2^+ groups are also created within the leached layers, this eventually resulting in the preferential removal of Al. The measured depths of Al preferential leaching in the plagioclase series also show a positive dependence on anorthite concentration (see Fig. 15, HELLMANN, 1995; based on data in CASEY et al., 1991).

These results concerning overall plagioclase dissolution rates and composition can be examined from several angles. First of all, as the anorthite content increases, the Al content increases concomitantly. This implies that at a given pH in the acid to neutral range, the surface concentration of >Al–OH_2^+ groups increases as a function of [Al] in the solid. Recalling that overall dissolution rates are proportional to surface charge (Eqns. 18, 19), the increase in positive surface charge due to increasing Al concentration (i.e. anorthite content) is probably one of the main reasons for the increased dissolution rate as a function of plagioclase composition at acid to neutral pH conditions (WALTHER, 1996). It has also been postulated that as the Al to Si ratio increases from 1:3 in albite to 1:1 in anorthite, the cation-oxygen bonds become weaker, and therefore the rates of dissolution should increase with increasing anorthite content (BRADY & WALTHER, 1989). Structural differences in the plagioclases also play a potentially important role. The albite structure (Ab_{97} - Ab_{100}) contains SiO_4 tetrahedra that are interconnected with each other; the loss of AlO_4 tetrahedra does not isolate the SiO_4 tetrahedra, rather a partially polymerized and stable network remains.

On the other hand, the anorthite structure (An_{73} - An_{100}) contains SiO_4 and AlO_4 tetrahedra on a regular alternating basis, due to the Al-avoidance rule. The plagioclases with compositions ranging from approximately An_{22} to An_{73} have an intermediate structure (DEER, HOWIE & ZUSSMAN, 1979). These structural and compositional differences in the plagioclase series imply that the loss of surface AlO_4 tetrahedra (i.e. >Al–OH_2^+ groups) will affect the kinetics of surface SiO_4 tetrahedra detachment (i.e. >SiOH groups).

The important point in the above argument is that the trend of increasingly isolated SiO_4 tetrahedra translates to an increased rate of dissolution (CASEY et al., 1991). The increased rate of dissolution, in turn, is due to the loss of structural continuity at the surface caused by the preferential loss of AlO_4 tetrahedra and the concomitant creation of detached and isolated SiO_4 tetrahedra. The same idea of isolated SiO_4 tetrahedra as discussed above has also been presented in terms of a bond hydrolysis argument: dissolution of albite requires the hydrolysis of both >Al–O_{br}–Si< and >Si–O_{br}–Si< bonds, whereas the dissolution of anorthite only requires the hydrolysis of weaker >Al–O_{br}–Si< bonds (OELKERS & SCHOTT, 1995). A final argument with respect to plagioclase dissolution rates is applicable to the plagioclase series ranging from albite to bytownite, but not including anorthite. Based on data presented in CASEY et al. (1991), HELLMANN (1995) determined that the rate of Si release (i.e. overall rate of dissolution) has a positive, non-linear dependence on the depth of Al preferential leaching. The fact that Al preferential leaching depths increase with *increasing* dissolution rates indicates that the preferential loss of AlO_4 tetrahedra (for the plagioclase series albite to bytownite) results in the formation of leached layers that are structurally stable. This suggests that isolated SiO_4 tetrahedra are not created, as would be the case for anorthite. The question then becomes what is the relationship between depths of leaching and overall dissolution rates? The loss of AlO_4 tetrahedra, as well as interstitial cations such as Na, K, and Ca, from within the leached zone serve to structurally ”open up” this altered zone, leaving it more permeable and susceptible to penetration by aqueous species, such as H^+ (see details on estimated increased rates of diffusion in leached zones in HELLMANN, 1995). The penetration of aqueous species into the leached structure may render a greater population of >Si–O_{br}–Si< and >Al–O_{br}–Si< framework bonds available to hydrolysis reactions, and this in turn, may serve to enhance the overall rate of dissolution. This argument is based on surface groups becoming detached not only from ”frontal attack” by hydrolysis reactions at the fluid-surface, but also via ”back attack” from within the leached zone. Thus, an increased number of hydrolysis reactions per surface group should translate to an overall greater rate of surface detachment, and hence a faster global rate of dissolution.

It is also possible to speculate that the retreat of the fluid/solid interface may not always occur via the uniform detachment of individual surface groups. An alternative to an uniform rate of detachment is based on the idea that hydrolysis reactions deep within a leached layer may lead to the rupture of a sufficient number of bonds such that a large fragment of the leached layer detaches itself from the bulk structure and is then subsequently dissolved in the solution. Such a mechanism requires a positive relationship between the depth of leached layers and their potential for detachment. Partial support of this idea is based on evidence of the fragile nature of leached layers, and the ease of their mechanical removal, as is discussed in the labradorite dissolution study of SCHWEDA et al. (1997).

The relation between leaching depths, Al content, Na^+, K^+, Ca^+-H^+ ion exchange, and the concentration of framework bonds susceptible to hydrolysis reactions may also be partially responsible for the pH-dependency of all feldspar dissolution rates. Thus, at acid pH conditions where significant leached layers are formed, dissolution rates should predictably be higher due to the increased availability of surface *and* near-surface framework bond hydrolysis sites. The interdependence of overall dissolution rates and depths of preferential leaching implies that dissolution is not strictly a 2-D surface process, but rather a 3-D volume process that involves reaction both at surface sites and at sites within the near-surface zone (HELLMANN 1995, 1997; HELLMANN et al., 1997; MUIR & NESBITT, 1997).

Conclusions

The application of many of the techniques derived from the rapidly changing field of surface science has led to many important advances in understanding the behavior of mineral-water interactions. It is becoming increasingly apparent that surface charge and speciation need to be an integral part of theories that describe not only equilibrium processes at fluid-mineral interfaces, but also the kinetics of these interfacial processes. An example of this is the formulation of kinetic rate laws that specifically formulate the rate dependence of dissolution or precipitation as a function of the adsorption of aqueous species on surfaces. Rate laws that incorporate adsorption processes have the potential for more accurately modeling water-mineral interactions.

As noted in BLUM & LASAGA (1988), surface charge and speciation data serve as an important tool in unifying dissolution rate data and dissolution mechanisms. As has been discussed in this and other studies, such diverse aspects of feldspar dissolution behavior as the pH dependence of dissolution rates, the preferential leaching of Al, H penetration into leached layers, and the relative rates of dissolution of the plagioclase series can be related to surface charge and speciation. One of the main challenges in the future will be understanding the relation between surface speciation and charge with respect to dissolution and precipitation rates of minerals and glasses in chemically complex solutions, as well as at elevated temperatures and pressures; this will necessitate advances in both experimental and theoretical approaches.

References

AMRHEIN, C. & SUAREZ, D. L. (1988): The use of a surface complexation model to describe the kinetics of ligand-promoted dissolution of anorthite. - Geochim. Cosmochim. Acta 52, 2785-2793.

ANDERSON D. L. (1989): Theory of the Earth. - Blackwell Scientific Publications.

ANDERSON, M. A. & RUBIN, A. J. (1981): Adsorption of Inorganics at Solid-Liquid Interfaces. - Anne Arbor Science, Ann Arbor, MI, 357p.

BERNER, R. A. (1992): Weathering, plants, and the long-term carbon cycle. - Geochim. Cosmochim. Acta 56, 3225-3231.

BLUM, A. E. & LASAGA, A. C. (1988): Role of surface speciation in the low-temperature dissolution of minerals. - Nature 331, 431-433.

BLUM, A. E. & LASAGA, A. C. (1991): The role of surface speciation in the dissolution of albite. - Geochim. Cosmochim. Acta 55, 2193-2201.

BRADY, P. V. & WALTHER, J. V. (1989): Controls on silicate dissolution rates in neutral and basic pH solutions at 25°C. - Geochim. Cosmochim. Acta 53, 2823-2830.

BUNKER, B. C., TALLANT, D. R., HEADLEY, T. J., TURNER, G. L., & KIRKPATRICK, R. J. (1988): The structure of leached sodium silicate glass. - Physics and Chemistry of Glasses 29, 106-120.

CASEY, W. H. & SPOSITO, G. (1992): On the temperature dependence of mineral dissolution rates. - Geochim. Cosmochim. Acta 56, 3825-3830.

CASEY, W. H., WESTRICH, H. R., & ARNOLD, G. W. (1988): Surface chemistry of labradorite feldspar reacted with aqueous solutions at pH = 2, 3, and 12. - Geochim. Cosmochim. Acta 52, 2795-2807.

CASEY, W. H., WESTRICH, H. R., ARNOLD, G. W. & BANFIELD, J. F. (1989): The surface chemistry of dissolving labradorite feldspar. - Geochim. Cosmochim. Acta 53, 821-832.

CASEY, W. H., WESTRICH, H. R., & HOLDREN, G. R. (1991): Dissolution rates of plagioclase at pH = 2 and 3. - Amer. Mineral. 76, 211-217.

CHOU, L. & WOLLAST, R. (1984): Study of the weathering of albite at room temperature and pressure with a fluidized bed reactor. - Geochim. Cosmochim. Acta 48, 2205-2217.

CHOU, L. & WOLLAST, R. (1985): Steady-state kinetics and dissolution mechanisms of albite. - Am. J. Sci. 285, 963-993.

CORRENS, C. W. & von ENGELHARDT, W. (1938): Neue Untersuchungen über die Verwitterung des Kalifeldspates. - Chemie der Erde 12, 1-22.

DEER, W. A., HOWIE, R. A. & ZUSSMAN, J. (1978): An Introduction to the Rock Forming Minerals. - Longman.

FORNI, L. (1973): Comparison of the methods for the determination of surface acidity of solid catalysts. - Catal. Rev. 8, 65-115.

GARRELS, R. M. & HOWARD, P. (1957): Reactions of feldspar and mica with water at low temperature and pressure. - Proc. 6th Natl. Conf. on Clays and Clay Minerals, pp. 68-88. Pergamon Press, Oxford.

GEISINGER, K. L., GIBBS, G.V. & NAVROTSKY, A. (1985): A molecular orbital study of bond length and angle variations in framework structures. - Phys. Chem. Minerals 11, 266-283.

HELGESON, H. C., MURPHY, W. M. & AAGAARD, P. (1984): Thermodynamic and kinetic constraints on reaction rates among minerals and aqueous solutions. II. Rate constants, effective surface area, and the hydrolysis of feldspar. - Geochim. Cosmochim. Acta 48, 2405-2432.

HELLMANN, R. (1994): The albite-water system: Part I. The kinetics of dissolution as a function of pH at 100, 200 and 300°C. - Geochim. Cosmochim. Acta 58, 595-611.

HELLMANN, R. (1995): The albite-water system: Part II. The time-evolution of the stoichiometry of dissolution as a function of pH at 100, 200 and 300°C. - Geochim. Cosmochim. Acta 59, 1669-1697.

HELLMANN, R. (1997): The albite-water system: Part IV. Diffusion modeling of leached and hydrogen-enriched layers. - Geochim. Cosmochim. Acta 61, 1595-1611.

HELLMANN, R. (submitted): Surface charge and speciation of albite and albite glass as a function of pH: the effects of surface composition and structure. - Geochim. Cosmochim. Acta

HELLMANN, R., DRAN, J.-C.& DELLA MEA, G. (1997): The albite-water system: Part III. Characterization of leached and hydrogen-enriched layers formed at 300°C using MeV ion beam techniques. - Geochim. Cosmochim. Acta 61, 1575-1594.

HELLMANN, R., EGGLESTON, C. M., HOCHELLA, M. F. Jr. & CRERAR, D. A. (1990): The formation of leached layers on albite surfaces during dissolution under hydrothermal conditions. - Geochim. Cosmochim. Acta 54, 1267-1281.

HOHL, H. & STUMM, W. (1976): Interaction of Pb^{+2} with hydrous γ-Al_2O_3. - J. Colloid Interface Sci. 55, 281-288.

HUANG, C. P. (1981): The surface acidity of hydrous solids. - In: Adsorption of Inorganics at Solid Solution Interfaces (eds. M. A. ANDERSON & A. J. RUBIN); pp. 183-217. Ann Arbor Science.

ILER, R. K. (1979): The Chemistry of Silica. - John Wiley & Sons.

KUMMERT, R. & STUMM, W. (1980): Surface complexation of organic acids on hydrous γ-Al_2O_3. - J. Colloid Interface Sci. 75, 373-385.

MOREL, F. M. M., WESTALL, J. C. & YEASTED, J. G. (1981): Adsorption models: A mathematical analysis in the framework of general equilibrium calculations. - In: Adsorption of Inorganics at Solid Solution Interfaces (eds. M. A. ANDERSON & A. J. RUBIN); pp. 263-294. Ann Arbor Science.

MUIR, I. J., BANCROFT, G. M., SHOTYK, W. & NESBITT, H. W. (1990): A SIMS and XPS study of dissolving plagioclase. - Geochim. Cosmochim. Acta 54, 2247-2256.

MUIR, I. J. & NESBITT, H. W. (1997): Reactions of aqueous anions and cations at the labradorite-water interface: Coupled effects of surface processes and diffusion. - Geochim. Cosmochim. Acta 61, 265-274.

OELKERS, E. H. & SCHOTT, J. (1995): The dependence of silicate dissolution rates on their structure and composition. - In: Water-Rock Interaction WRI-8 (eds. Y. K. KHARAKA & O. V. CHUDAEV); pp. 153-156. Balkema.

OXBURGH, R., DREVER, J. I. & SUN, Y.-T. (1994): Mechanism of plagioclase dissolution in acid solution at 25°C. - Geochim. Cosmochim. Acta 58, 661-669.

PARKS, G. A. (1965): The isoelectric points of solid oxides, solid hydroxides, and aqueous hydroxo-complex systems. - Chemical Reviews 65, 177-198.

PARKS, G. A. (1967): Aqueous surface chemistry of oxides and complex oxide minerals. - In: Equilibrium Concepts in Natural Water Systems; Amer. Chem. Soc. Adv. Chem. Ser. 67, pp. 121-160.

PEDERSON, L. R., BAER, D. R., McVAY, G. L. & ENGELHARD, M. H. (1986): Reaction of soda-lime silicate glass in isotopically labelled water. - Journal of Non-Crystalline Solids 86, 369-380.

PETIT, J.-C., DELLA MEA, G., DRAN, J.-C., MAGONTHIER, M.-C., MANDO, P. A. & PACCAGNELLA, A. (1990): Hydrated layer formation during dissolution of complex silicate glasses and minerals. - Geochim. Cosmochim. Acta 54, 1941-1955.

PETIT, J.-C., DRAN, J.-C., DELLA MEA, G. & PACCAGNELLA, A. (1989): Dissolution mechanisms of silicate minerals yielded by intercomparison with glasses and radiation damage studies. - Chem. Geol. 78, 219-227.

PULFER, K., SCHINDLER, P. W., WESTALL, J. C.& GRAUER, R. (1984): Kinetics and mechanism of dissolution of bayerite (γ-$Al(OH)_3$) in HNO_3-HF solutions at 298.2°K. - J. Colloid Interface Sci. 101, 554-564.

SAHAI, N. & SVERJENSKY, D. A. (1997): Evaluation of internally consistent parameters for the triple-layer model by the systematic analysis of oxide surface titration data. - Geochim. Cosmochim. Acta 61, 2801-2826.

SCHINDLER, P. W. (1981): Surface complexes at oxide-water interfaces. - In: Adsorption of Inorganics at Solid Solution Interfaces (eds. M. A. ANDERSON & A. J. RUBIN); pp. 1-47. Ann Arbor Science.

SCHINDLER, P. W. & STUMM, W. (1987): The surface chemistry of oxides, hydroxides, and oxide minerals. - In: Aquatic Surface Chemistry (ed. W. STUMM); pp. 83-110. John Wiley & Sons.

SCHOTT, J. (1990): Modeling of the dissolution of strained and unstrained multiple oxides: the surface speciation approach. - In: Aquatic Chemical Kinetics (ed. W. STUMM); pp. 337-365. John Wiley & Sons, Inc.

SCHWEDA, P. (1990): Kinetics and mechanisms of alkali feldspar dissolution at low temperatures. - Ph.D. dissertation, Stockholms Universitets Institution för Geologi och Geokemi.

SCHWEDA, P., SJÖBERG, L., & SÖDERVALL, U. (1997): Near-surface composition of acid-leached labradorite investigated by SIMS. - Geochim. Cosmochim. Acta 61, 1985-1994.

STILLINGS, L. L. & BRANTLEY, S. L. (1995): Feldspar dissolution at 25°C and pH 3: Reaction stoichiometry and the effect of ionic strength. - Geochim. Cosmochim. Acta 59, 1483-1496.

STILLINGS, L. L., BRANTLEY S. L., & MACHESKY, M. L. (1995): Proton adsorption at an adularia feldspar surface. - Geochim. Cosmochim. Acta 59, 1473-1482.

STUMM, W. & FURRER, G. (1987): The dissolution of oxides and aluminum silicates; examples of surface-coordination-controlled kinetics. - In: Aquatic Surface Chemistry (W. STUMM, ed.), pp. 197-219, John Wiley and Sons, N.Y.

TAMM, V. O. (1930): Experimentelle Studien über die Verwitterung und Tonbildung von Feldspäten. - Chemie der Erde 4, 420-430.

UNWIN & BARD (1992): Ultramicroelectrode voltammetry in a drop of solution: a new approach to the measurement of adsorption isotherms at the solid-liquid interface. - Anal. Chem. 64, 113-119.

WALTHER, J. V. (1996): Relation between rates of aluminosilicate mineral dissolution, pH, temperature, and surface charge. - Am. J. Sci. 296, 693-728.

WALTHER, J. V., BRANTLEY, S. L., & STILLINGS, L. L. (1997): Comment and Reply: Feldspar dissolution at 25°C and low pH. - Am. J. Sci. 297, 1012-1032.

WOLERY, T. J. (1983): EQ3NR, A Computer Program for Geochemical Aqueous Speciation-Solubility Calculations: User's Guide and Documentation.

XIAO, Y. & LASAGA, A. C. (1994): Ab initio quantum mechanical studies of the kinetics and mechanisms of silicate dissolution: H^+ (H_3O^+) catalysis. - Geochim. Cosmochim. Acta 58, 5379-5400.

ZINDER, B., FURRER, G., & STUMM, W. (1986): The coordination chemistry of weathering: II. Dissolution of Fe(III) oxides. - Geochim. Cosmochim. Acta 50, 1861-1869.